

**ANALYSIS OF THE RECORDED RESPONSE
OF LEXINGTON DAM DURING VARIOUS LEVELS
OF GROUND SHAKING**

by

Faiz I. Makdisi, C.-Y. Chang, Z.-L. Wang and C.-M. Mok

**Geomatrix Consultants
100 Pine Street, 10th Floor
San Francisco, California**

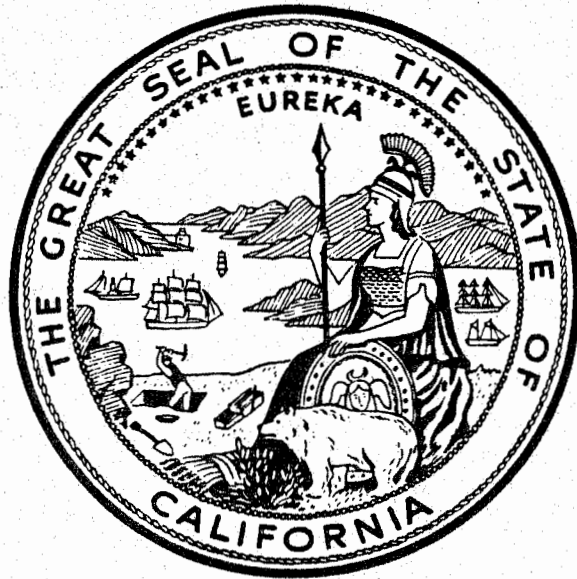
Data Utilization Report CSMIP/94-03

California Strong Motion Instrumentation Program

March 1994

This study was conducted at the Geomatrix Consultants in San Francisco and was supported by the Department of Conservation under Contract No. 1090-508.

**California Department of Conservation
Division of Mines and Geology
Office of Strong Motion Studies
801 K Street, MS 13-35
Sacramento, California 95814-3531**



DIVISION OF MINES AND GEOLOGY
JAMES F. DAVIS
STATE GEOLOGIST

DISCLAIMER

The content of this report was developed under Contract No. 1090-501 from the Strong Motion Instrumentation Program in the Division of Mines and Geology of the California Department of Conservation. This report has not been edited to the standards of a formal publication. Any opinions, findings, conclusions or recommendations contained in this report are those of the authors, and should not be interpreted as representing the official policies, either expressed or implied, of the State of California.

PREFACE

The California Strong Motion Instrumentation Program (CSMIP) in the Division of Mines and Geology of the California Department of Conservation promotes and facilitates the improvement of seismic codes through the Data Interpretation Project. The objective of the this project is to increase the understanding of earthquake strong ground shaking and its effects on structures through interpretation and analysis studies of CSMIP and other applicable strong motion data. The ultimate goal is to accelerate the process by which lessons learned from earthquake data are incorporated into seismic code provisions and seismic design practices.

The specific objectives of the CSMIP Data Interpretation Project are to:

1. Understand the spatial variation and magnitude dependence of earthquake strong ground motion.
2. Understand the effects of earthquake motions on the response of geologic formations, buildings and lifeline structures.
3. Expedite the incorporation of knowledge of earthquake shaking into revision of seismic codes and practices.
4. Increase awareness within the seismological and earthquake engineering community about the effective usage of strong motion data.
5. Improve instrumentation methods and data processing techniques to maximize the usefulness of SMIP data. Develop data representations to increase the usefulness and the applicability to design engineers.

This report is the eighth in a series of CSMIP data utilization reports designed to transfer recent research findings on strong-motion data to practicing seismic design professionals and earth scientists. CSMIP extends its appreciation to the members of the Strong Motion Instrumentation Advisory Committee and its subcommittees for their recommendations regarding the Data Interpretation Research Project.

Moh J. Huang
CSMIP Data Interpretation
Project Manager

Anthony F. Shakal
CSMIP Program Manager

ABSTRACT

The recordings at Lexington Dam, due to at least three different levels of shaking, provided excellent data for examining the validity of commonly used dynamic analysis procedures as well as examining nonlinear stress-strain behavior of the dam material due to earthquake shaking. The properties of the embankment materials including cross-hole shear wave velocity measurements were well documented during earlier safety evaluation studies.

Amplification ratios of peak ground acceleration between the crest and abutment rock recordings decreased with increasing levels of ground shaking. For abutment rock acceleration levels of about 0.03 to 0.04g, the amplification ratio is about 3 to 4; at acceleration levels of about 0.1g, the amplification ratio is about 1.5 to 2, and at acceleration levels of about 0.4 to 0.45g, the amplification is about 1.0.

This report summarizes the results of Fourier spectral analyses of the recordings at the dam crest and rock abutment for the three earthquakes described above; and one- and two-dimensional dynamic response analyses to evaluate the nonlinear strain-dependent behavior of the embankment materials at various levels of earthquake shaking. Response and Fourier spectral ratios (crest to abutment) of the recorded ground motions showed a definite shift in the fundamental natural period of the embankment with increased level of shaking. Two-dimensional finite element analyses of the embankment response provided predictions of motions at the crest of the dam that are in reasonable agreement with recorded motions. The results of the finite element computations showed a non-linear strain dependent behavior of the embankment materials for levels of shaking associated with the Loma Prieta earthquake.

APPLICATION TO CODES AND PRACTICES

Current guidelines for the evaluation of seismic stability of high embankment dams, located in active seismic environments, require the use of two-dimensional finite element dynamic analyses for estimating the embankment response. The analyses performed in this study showed that currently used dynamic analyses procedures, using the equivalent linear method to model the nonlinear strain-dependent behavior of the embankment material, can provide response estimates that are in reasonable agreement with the recorded data.

ACKNOWLEDGEMENTS

The contents of this report were developed under contract No. 1090-508 from the California Department of Conservation, Division of Mines and Geology, Strong Motion Instrument Program. However, those contents do not necessarily represent the policy of that agency nor endorsement by the State of California. The support of the Strong Motion Instrumentation Program is gratefully acknowledged. The authors also wish to thank Bob Teppel of the Santa Clara Valley Water District for providing valuable data on Lexington Dam, and the staff of the California Department of Water Resources, Division of Safety of Dams, for assisting our review of their files.

TABLE OF CONTENTS

	<u>Page</u>
1 INTRODUCTION	1
2 DESCRIPTION OF LEXINGTON DAM	3
3 ANALYSIS OF RECORDED GROUND MOTIONS	6
4 ANALYSES OF EMBANKMENT RESPONSE	41
4.1 Two-Dimensional Finite Element Analyses	41
4.1.1 Effects of Modulus and Damping Relationships	43
4.1.2 Effect of Depth to Rigid Boundary	44
4.2 ONE-DIMENSIONAL ANALYSES	46
5 SUMMARY AND CONCLUSIONS	60
REFERENCES	

1 INTRODUCTION

During the 1989 Loma Prieta earthquake (M_L 7), Lexington Dam, a 205-ft-high embankment located about 3 miles from the rupture surface, was subjected to strong ground shaking. Peak ground accelerations recorded at its abutment rock were about 0.4 g; peak accelerations recorded at the crest of the dam ranged from about 0.4 to 0.45 g.

During 1988 and 1989, the same embankment was shaken by two smaller events that had magnitudes M_L of 5.0 and 5.2. These events, which had epicenters in the Lake Elsmar area, occurred about 5 and 6 miles from the damsite. A map showing the locations of Lexington Dam and the epicenters of the three earthquakes is presented on Figure 1(a). Recorded peak accelerations at the damsite from the Lake Elsmar events ranged from about 0.04 to 0.08 g at the abutment rock and 0.18 to 0.22 g at the crest of the embankment. The recordings of these various levels of ground shaking at Lexington Dam provide an opportunity to evaluate the nonlinear, strain-dependent behavior of the embankment material in response to strong earthquake shaking, and to examine the ability of current dynamic analysis procedures to simulate the recorded response of the embankment. This report summarizes our analyses of the recordings at the dam crest and abutment for two of the three earthquakes described above. The analyses included computations of Fourier and response spectra as well as spectral ratios (crest to abutment) to examine the natural period of the embankment under various levels of ground shaking; and one- and two-dimensional dynamic response analyses to evaluate the nonlinear, strain-dependent behavior of the embankment materials at two levels of earthquake shaking. The report is organized into the following sections: Section 2 provides a description of the Lexington Dam embankment and material properties; Section 3 presents our analysis of recorded ground motions; Section 4 describes our analyses of embankment response; and Section 5 gives a summary and conclusions.

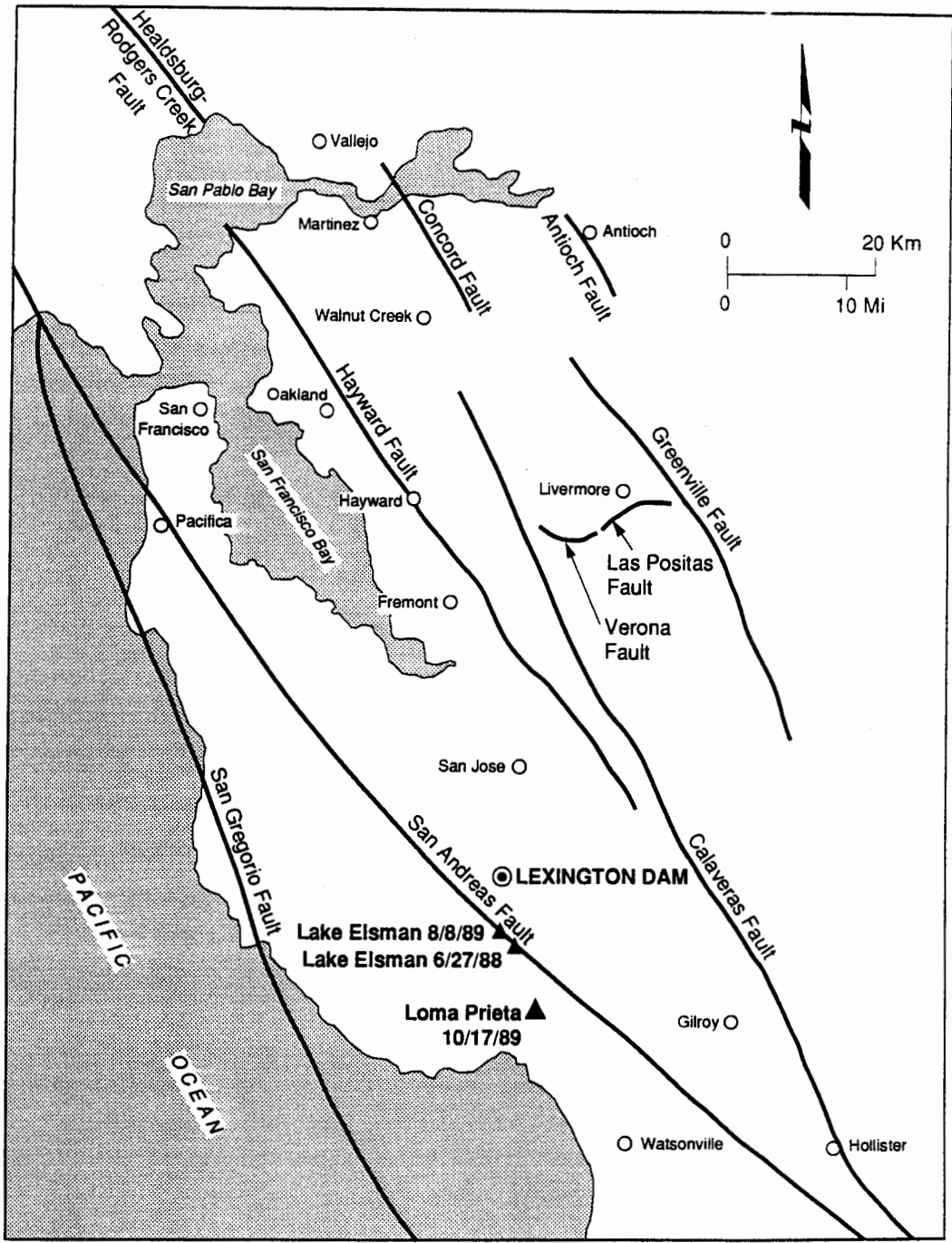


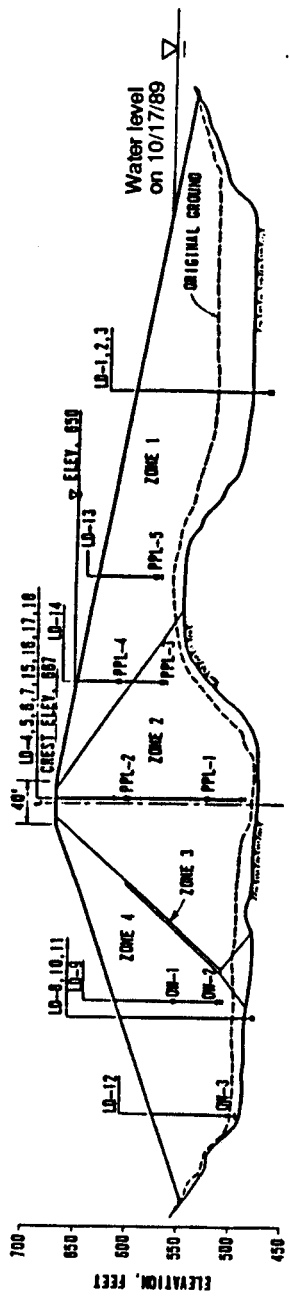
Figure 1(a): Map Showing Locations of Earthquake Epicenters Relative to Lexington Dam

2 DESCRIPTION OF LEXINGTON DAM AND ITS PERFORMANCE DURING THE LOMA PRIETA EARTHQUAKE

Lexington Dam sits on the east flank of the Santa Cruz Mountains, off Highway 17, about 17 miles north of Santa Cruz. The dam is 205 ft high and has a crest length of 810 ft. The dam was built in 1953. It is a zoned compacted earthfill embankment that has a downstream slope of 3:1 (H:V) and an upstream slope of 5½:1. A cross section through the maximum section of the embankment is shown on Figure 1(b). The embankment consists of four zones: upstream and downstream shells of gravelly clayey sands (Zones 1 and 4), a thick core of sandy gravelly clay (Zone 2), and an internal drain zone between the core and downstream shell (Zone 3). The downstream shell contains about 15% to 35% fines, the upstream shell about 20% to 65%. In both cases the fines are medium-plasticity clays having LL = 33 to 39 and PI = 14 to 24. The core, below a depth of 80 ft, is composed of 85% fines of medium to high plasticity (LL = 61 to 67 and PI = 38 to 44). Between the crest and a depth of 80 ft, the core material resembles the upstream shell material, having about 30% to 50% fines of medium plasticity (LL = 31 to 39 and PI = 14 to 18).

The foundation and abutments consist of bedrock of the Franciscan formation, which is composed chiefly of interbedded sandstone and shale, greenstone, and minor amounts of chert and schist. The topsoil at the foundation area was stripped prior to dam construction.

During the Loma Prieta earthquake the water level of Lexington Reservoir was about 100 feet below the crest of the dam (Volpe and Associates, 1990). The strong ground shaking at the dam site caused the crest of the embankment to settle about 0.85 feet at the maximum section. A maximum of 0.25 feet of lateral movement was measured in the downstream direction (Volpe and Associates, 1990). Transverse cracking was observed on both the upstream and downstream sides of both abutments, as well as longitudinal cracking on the upstream and downstream slopes of the embankment. The cracks were generally



SECTION

NOTE: DEPTHS OF THE BOREHOLES SHOWN ARE PROJECTED DEPTHS (SOME HOLES ARE NOT ON THE SECTION SHOWN).



KEY

↓ DEPTH OF BOREHOLE

⊕ PIEZOMETER TIP

○ OPEN WELL PIEZOMETER

⊖ PNEUMATIC PIEZOMETER

(from W. A. Wahler Associates, 1982)

Figure 1(b): Cross-Section Through Lexington Dam Showing Zones of Embankment

less than $\frac{1}{4}$ of an inch wide and extended between 2 and 7 feet deep (Volpe and Associates, 1990).

3 ANALYSIS OF RECORDED GROUND MOTIONS

As part of the California Division of Mines and Geology's Strong Motion Instrumentation Program, Lexington Dam was instrumented with three sets of strong motion accelerographs. One set is located at a rock outcrop at the left abutment (west of the concrete spillway); two sets located on the crest are intended to measure the response of the embankment. The locations of these instruments are shown on a topographic layout of the dam presented on Figure 1(c). At each location the accelerographs were oriented in three orthogonal directions: transverse (normal to the dam axis, component N00E); longitudinal (along the dam axis, component N90E); and vertical. During the Loma Prieta (M_L 7) earthquake of October 17, 1989, peak accelerations (in the transverse direction) of 0.39 and 0.45 g were recorded at the left and right crest of the dam, respectively; 0.45 g was recorded at the rock formation of the left abutment. The instruments at the damsite also triggered during two smaller magnitude (M_L ~5) earthquakes that had epicenters located near Lake Elsmar. One event occurred on June 27, 1988, the second on August 8, 1989. Peak accelerations at the damsite recorded in the transverse direction during these events were significantly lower than those of the Loma Prieta earthquake: 0.11 to 0.16 g on the crest and 0.03 g at the left abutment for the event of June 27, 1988; 0.16 to 0.18 g on the crest and 0.08 g at the left abutment for the earthquake of August 8, 1989. Peak ground accelerations for all three components and the earthquake dates are given in Table 1.

The recordings from these earthquakes were digitized by the staff of the Strong Motion Instrumentation Program (Shakal et al., 1989). The time histories of acceleration for each of the three earthquakes are presented as Figures 2(a) through 2(c). The time histories are shown for the three components at the left abutment bedrock and at the two crest locations. Similar plots of the time histories of velocity are shown on Figures 3(a) through 3(c), and of displacements on Figures 4(a) through 4(c).

TABLE 1
RECORDED PEAK ACCELERATIONS AT
LEXINGTON DAM DURING THREE EARTHQUAKES

Earthquake (Date)	Magnitude (M _L)	Approximate Distance to Rupture Zone (miles)	Peak Acceleration (g)		
			Left Abutment	Left Crest	Right Crest
Loma Prieta (Oct. 17, 1989)	6.9	3.7	E-W: 0.41 Up: 0.15 N-S: 0.08	0.40 0.22 0.18	0.34 0.10 0.45
Lake Elsman (Aug. 8, 1989)	5.2	11.2	E-W: 0.11 Up: 0.03 N-S: 0.08	0.17 0.08 0.18	0.22 0.10 0.16
Lake Elsman (June 27, 1988)	5.0	11.8	E-W: 0.04 Up: 0.02 N-S: 0.03	0.11 0.07 0.11	0.12 0.07 0.16

We computed acceleration response spectra, Fourier spectra, and Fourier spectral ratios (crest to abutment) for the recorded ground motions of the three earthquakes described above. The response spectra (5% damping) for each of the three components at each of the three recording instruments at the damsite are presented on Figure 5(a) for the Loma Prieta earthquake and Figures 5(b) and 5(c) for the two Lake Elsman events. The corresponding Fourier spectra for the same recordings are presented as Figure 6(a) through 6(c). Our analyses of the embankment response focused on the component of motion in the direction transverse to the dam axis, because potential deformations in this direction can significantly affect the stability of the embankment. The spectra on Figures 5(a) and 6(a) show that the first natural period of the embankment (in the transverse direction) during the Loma Prieta earthquake was about 1.0 to 1.1 seconds. The spectra on Figures 5(b) and 6(b) show that for the Lake Elsman event of August 8, 1989, the first natural period was about 0.4 to 0.5 seconds. The corresponding period during the Lake Elsman event of June 27, 1988, was about 0.3 to 0.5 seconds (Figures 5(c) and 6(c)). This comparison shows that the natural period of the embankment increased with increased levels of ground shaking (see Table 1). An increase

in the natural period with an increase in level of shaking reflects a decrease in the shear modulus of the site material (Chang et al., 1989).

The spectral ratios of recordings at the two crest locations and recordings at the left abutment bedrock are plotted on Figures 7 and 8 for the Loma Prieta earthquake. Figures 7(a) and 7(b) show the ratios of Fourier amplitude spectra (both unsmoothed and smoothed) for the two crest locations. Smoothing of the Fourier spectra was performed in the frequency domain at 1-Hz intervals using a triangular weighing function. Figures 8(a) and 8(b) show the corresponding ratios of the 5% damped response spectra. Figures 7(a) and 8(a) show that at the right crest location, the first natural period of the embankment in the transverse direction (component 000) is about 1.3 seconds. Similar plots are shown on Figures 9 and 10 for the Lake Elsmar event of August 8, 1989, and Figures 11 and 12 for the Lake Elsmar event of June 27, 1988. These figures show that, at the right crest location, the first natural period of the embankment in the transverse direction is about 0.5 seconds for the events of August 8, 1989, and June 27, 1988. Summary plots for the spectral ratios (crest to abutment) for all three events are shown on Figure 13 for the 5% damped response spectra and on Figure 14 for the Fourier amplitude spectra. Again, for the transverse component (component 000), the shift (increase) in the natural period with the increase in level of shaking is clear, as is the decrease in spectral amplification ratio. It should be noted that the level of shaking (in the transverse direction) represented by the peak ground acceleration at the left abutment bedrock for the two smaller Lake Elsmar events was 0.03 to 0.08 g, compared to 0.45 g for the Loma Prieta event. The increase in the fundamental period of the embankment suggests a significant reduction in shear modulus of the embankment material under Loma Prieta earthquake conditions.

Examination of the records from the June 27, 1988, Lake Elsmar event reveals that the instruments triggered late, and records of the early portion of ground motions may be lacking. Accordingly, this set of records was not

used in the dynamic response computations described in subsequent sections of this report. Plots of the 5% damped response spectra recordings from the two larger events are presented on Figure 15. The spectra are shown (for the transverse component) for the left abutment rock recording and for the right crest location. This location coincides with the maximum section shown on Figure 1, which will be used in the two-dimensional dynamic response analysis. Ratios of the Fourier amplitude spectra of the right crest recordings to those of the left abutment bedrock are shown on Figure 16.

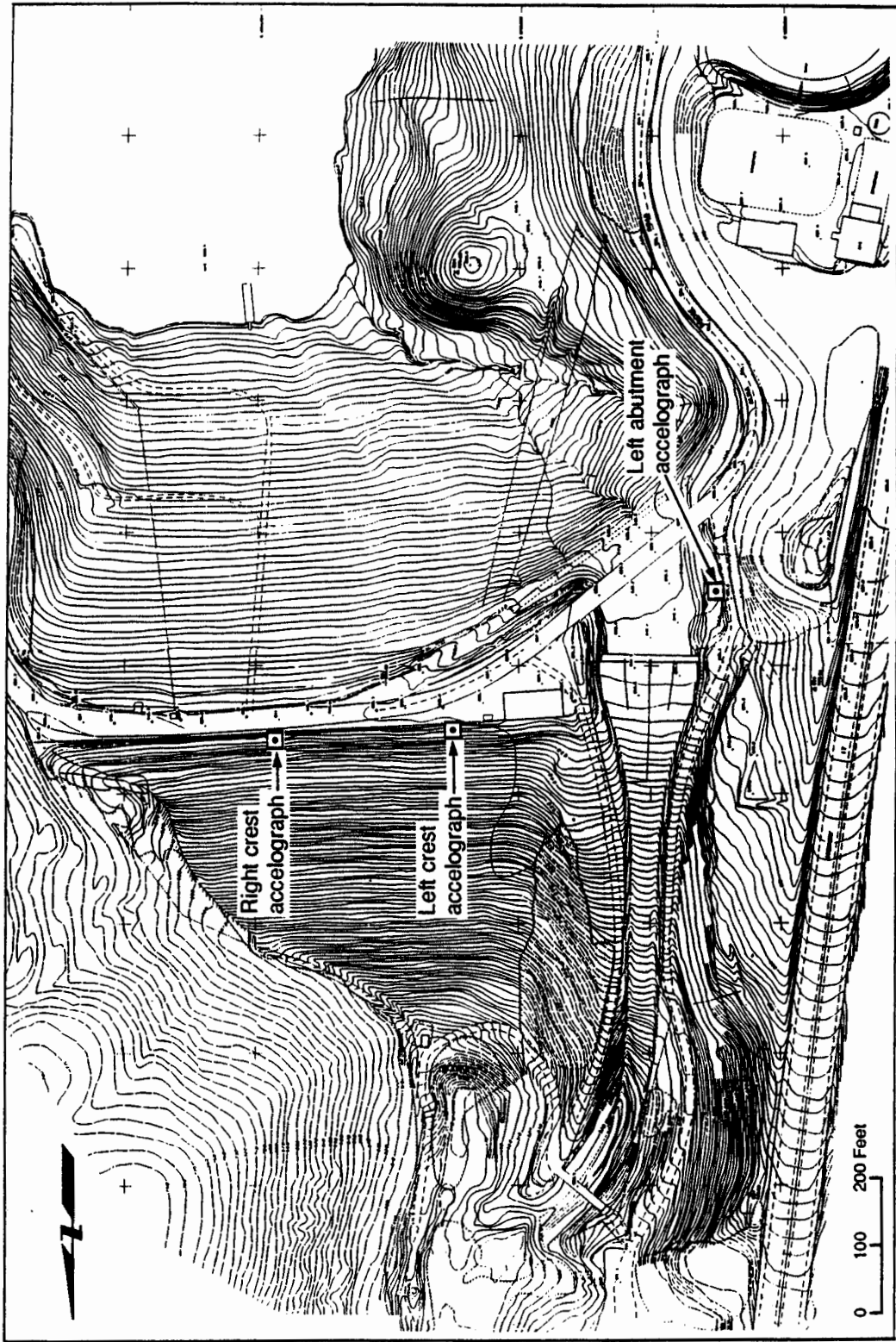


Figure 1(c): Plan of Lexington Dam Showing Locations of Recording Instruments

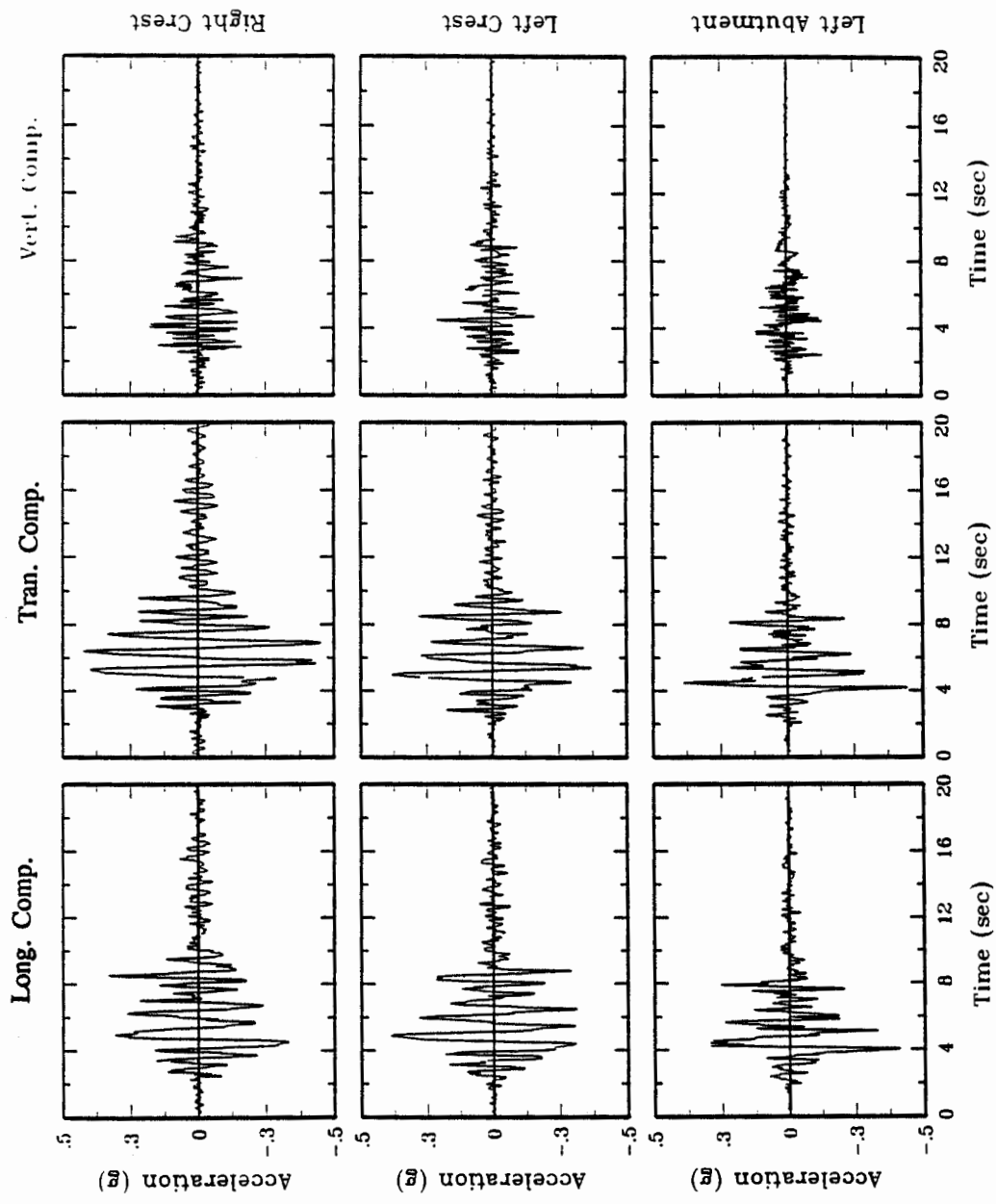


Figure 2(a): Acceleration Time Histories Recorded at Lexington Dam During the Loma Prieta Earthquake of October 17, 1989

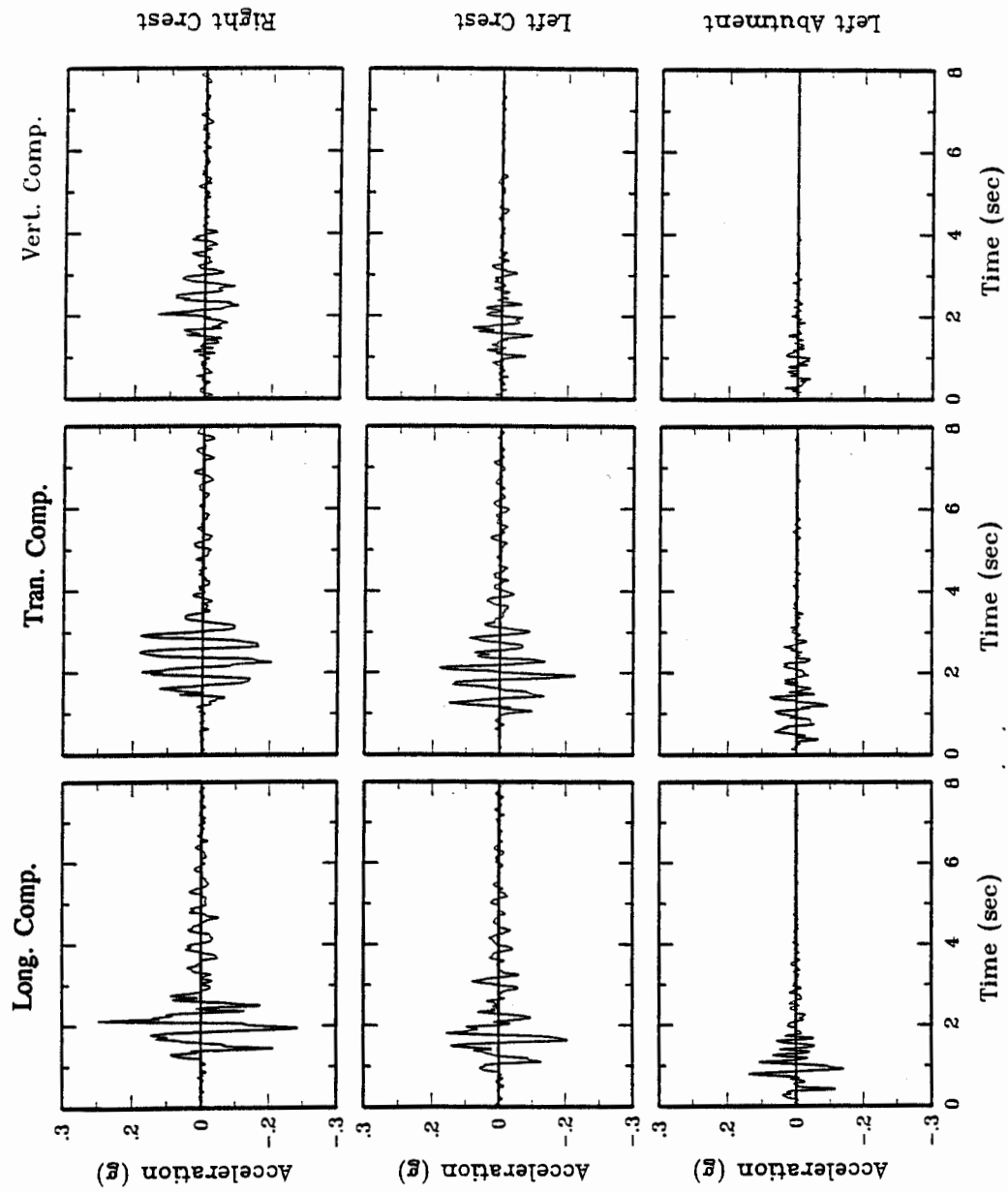


Figure 2(b): Acceleration Time Histories Recorded at Lexington Dam During the Lake Elsmann Earthquake of August 8, 1989

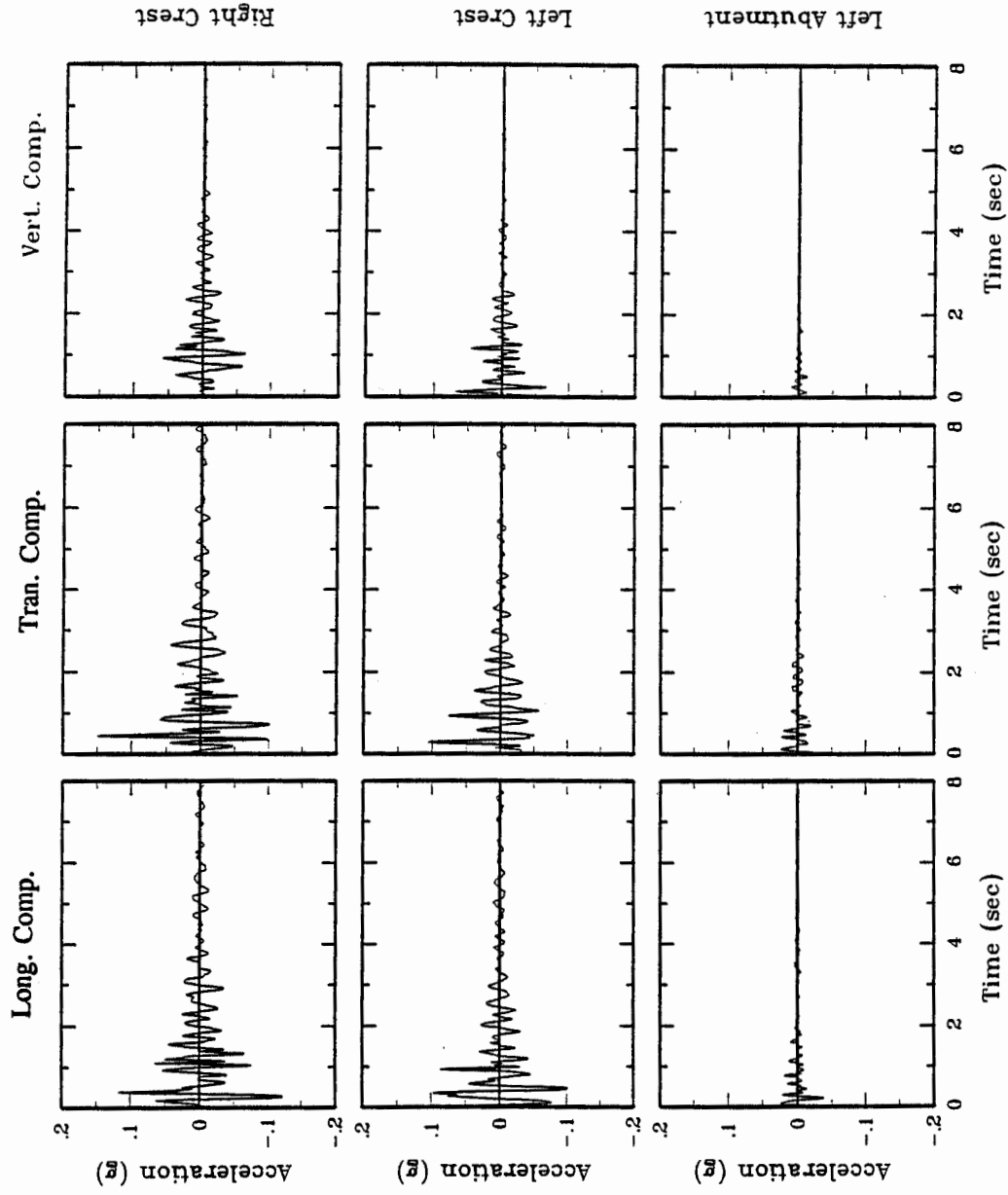


Figure 2(c): Acceleration Time Histories Recorded at Lexington Dam During the Lake Elsman Earthquake of June 27, 1988

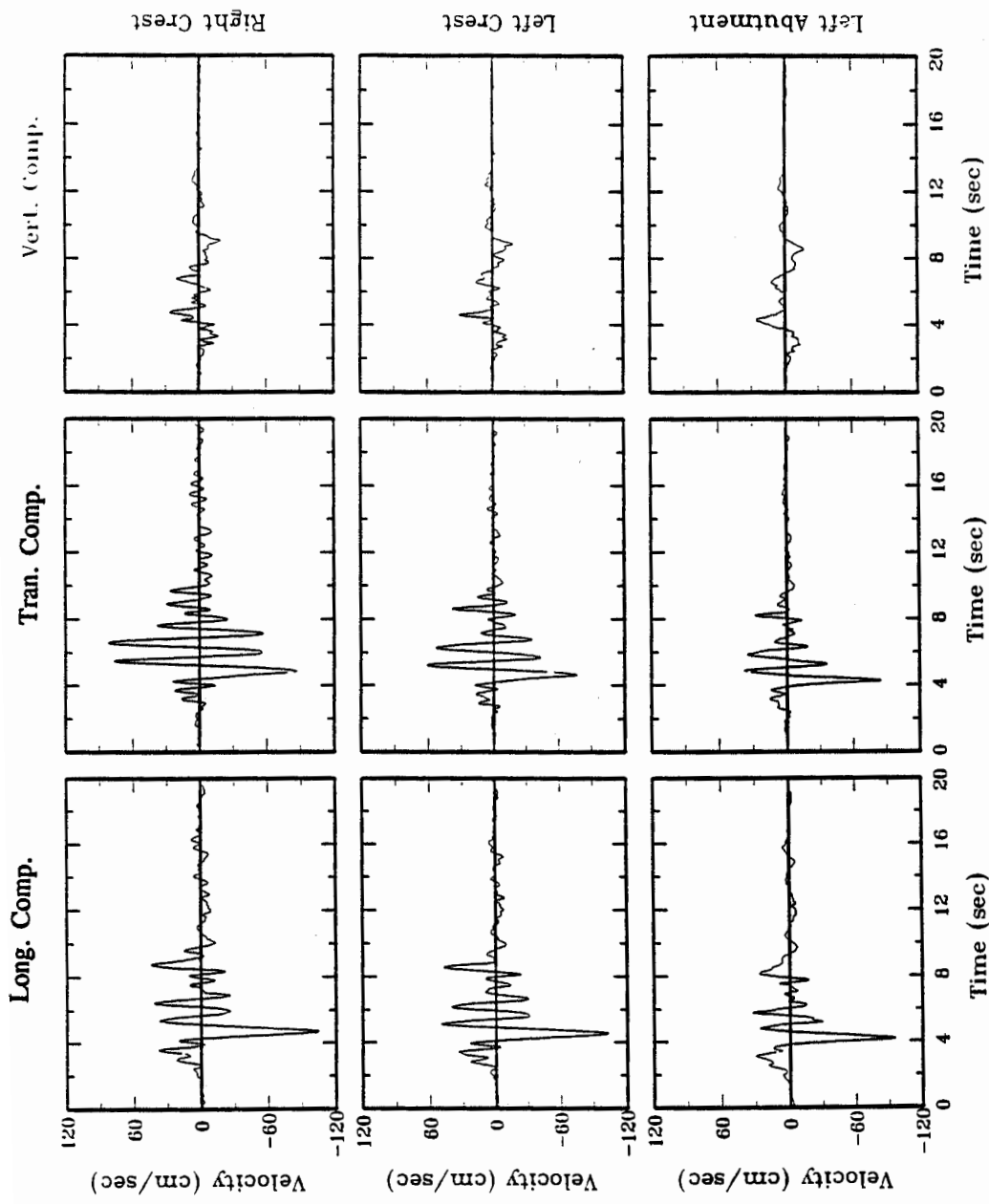


Figure 3(a): Velocity Time Histories Recorded at Lexington Dam During the Loma Prieta Earthquake of October 17, 1989

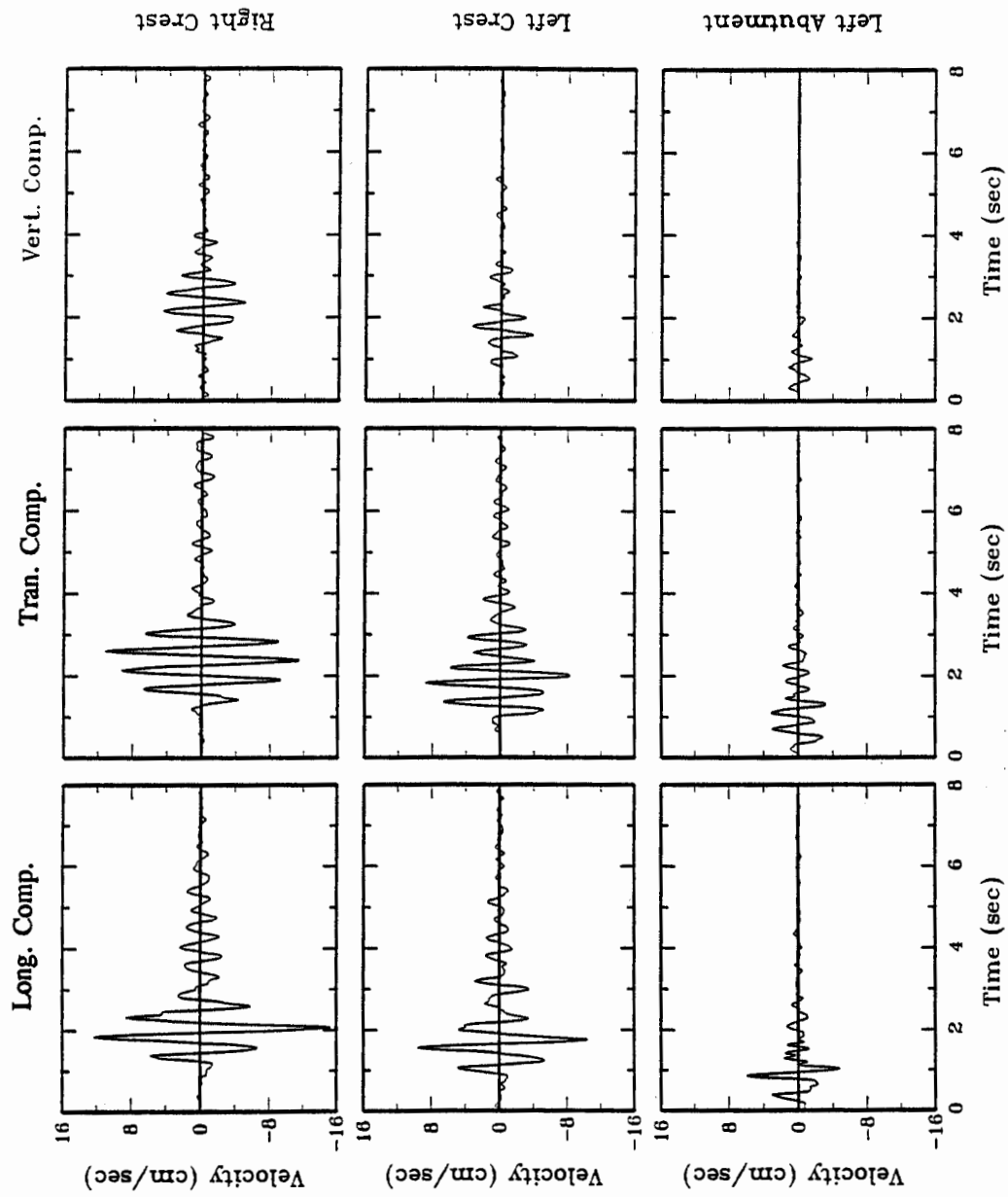


Figure 3(b): Velocity Time Histories Recorded at Lexington Dam During the Lake Elsman Earthquake of August 8, 1989

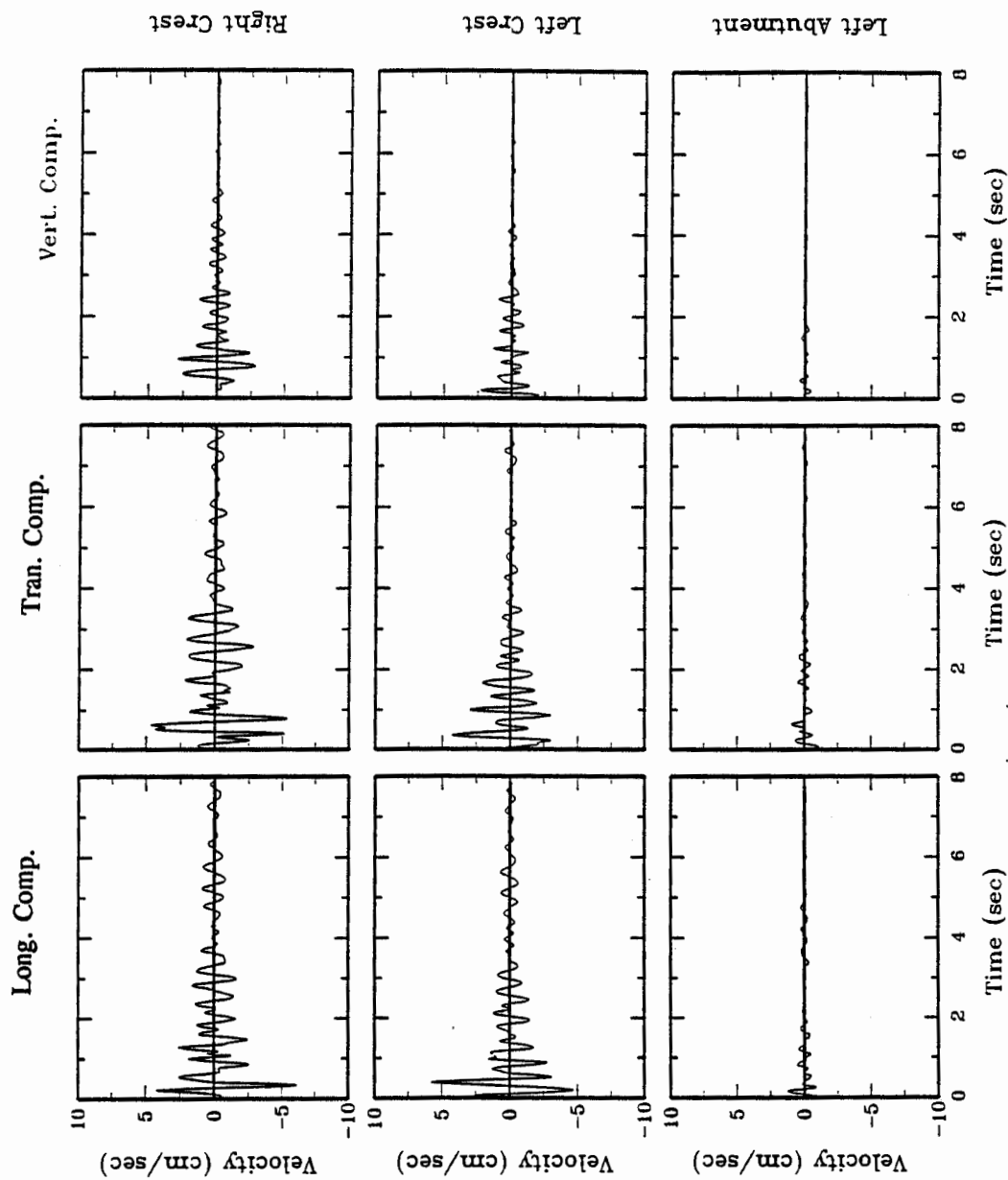


Figure 3(c): Velocity Time Histories Recorded at Lexington Dam During the Lake Elsman Earthquake of June 27, 1988

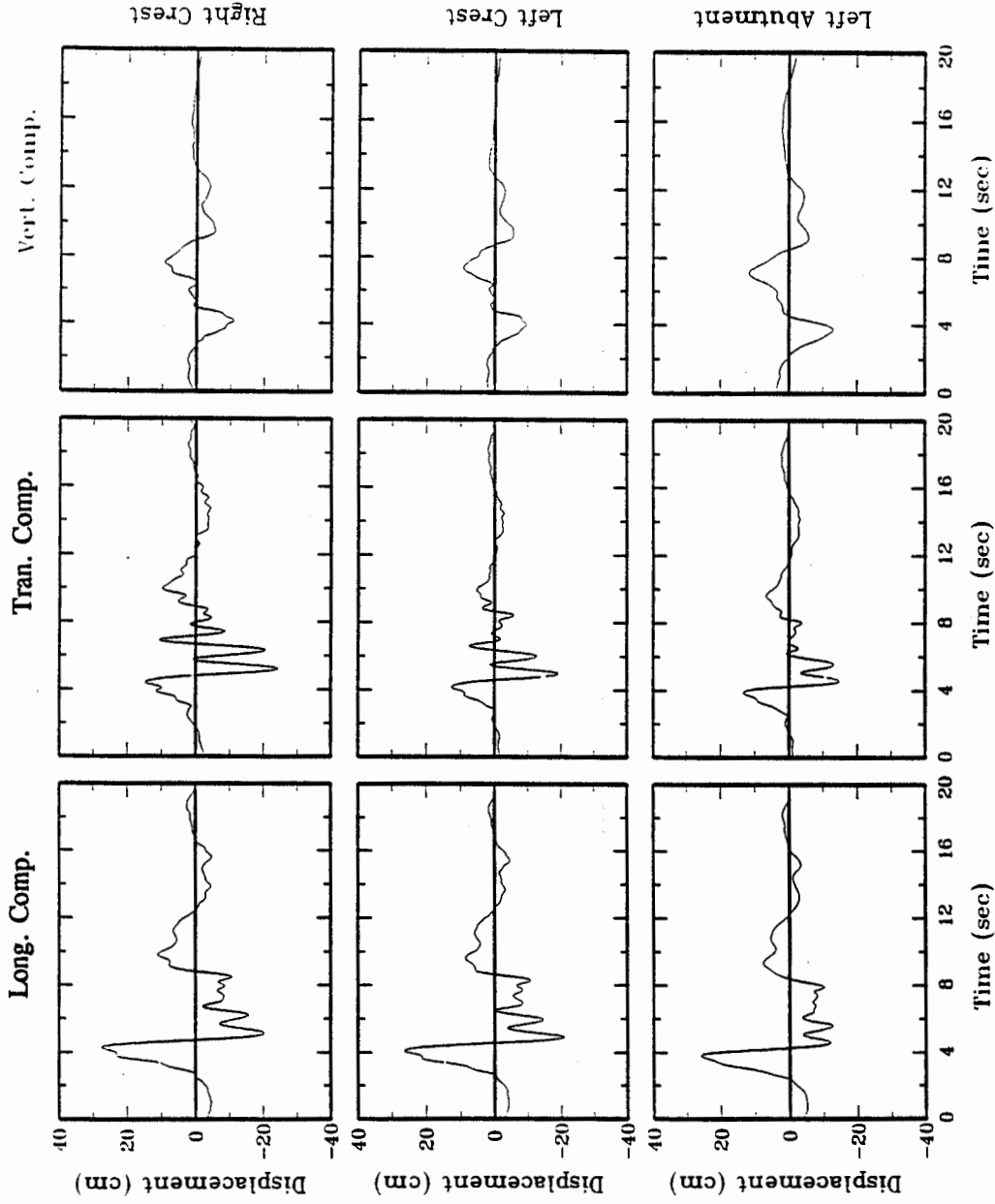


Figure 4(a): Displacement Time Histories Recorded at Lexington Dam During the Loma Prieta Earthquake of October 17, 1989

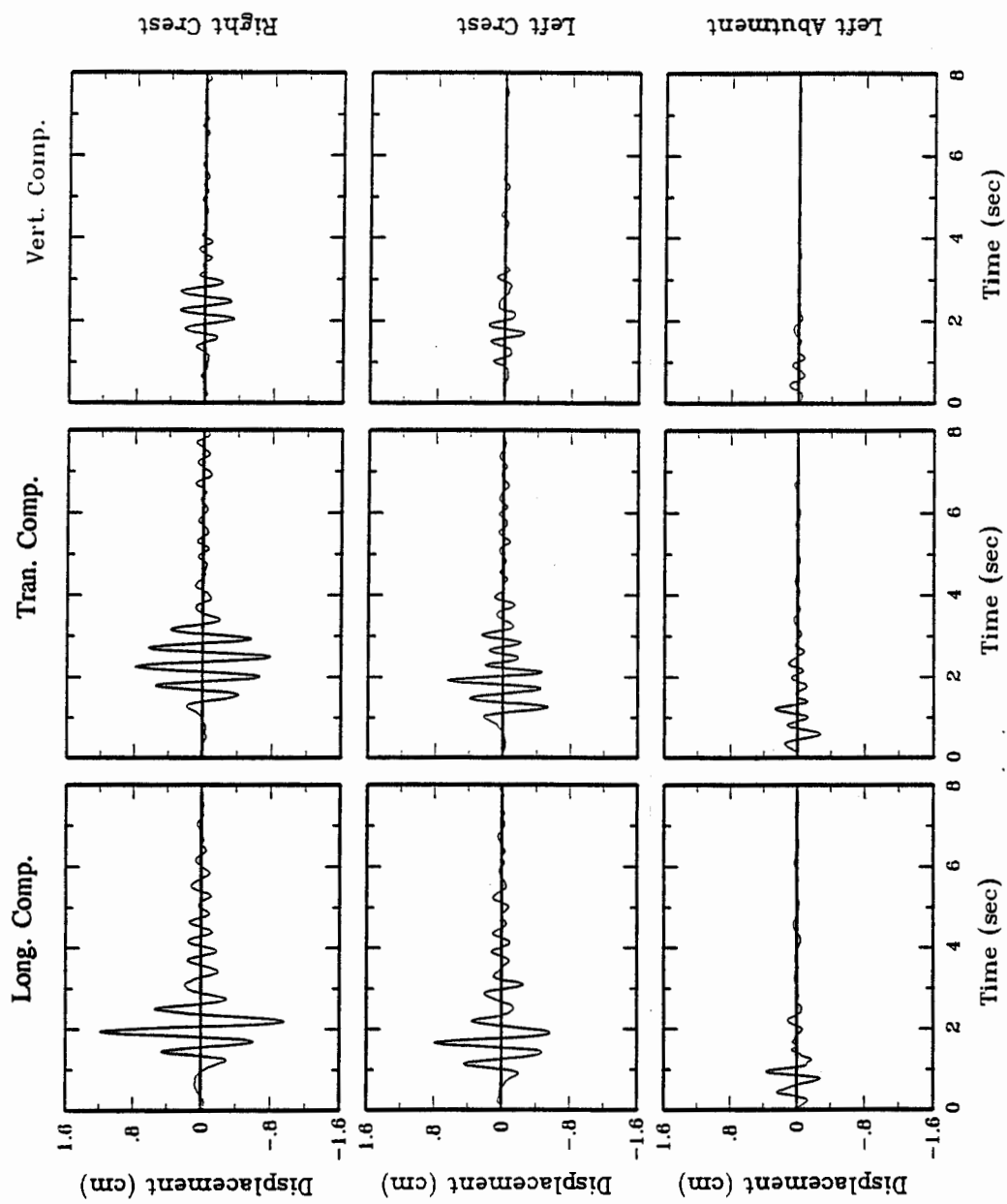


Figure 4(b): Displacement Time Histories Recorded at Lexington Dam During the Lake Elseman Earthquake of August 8, 1989

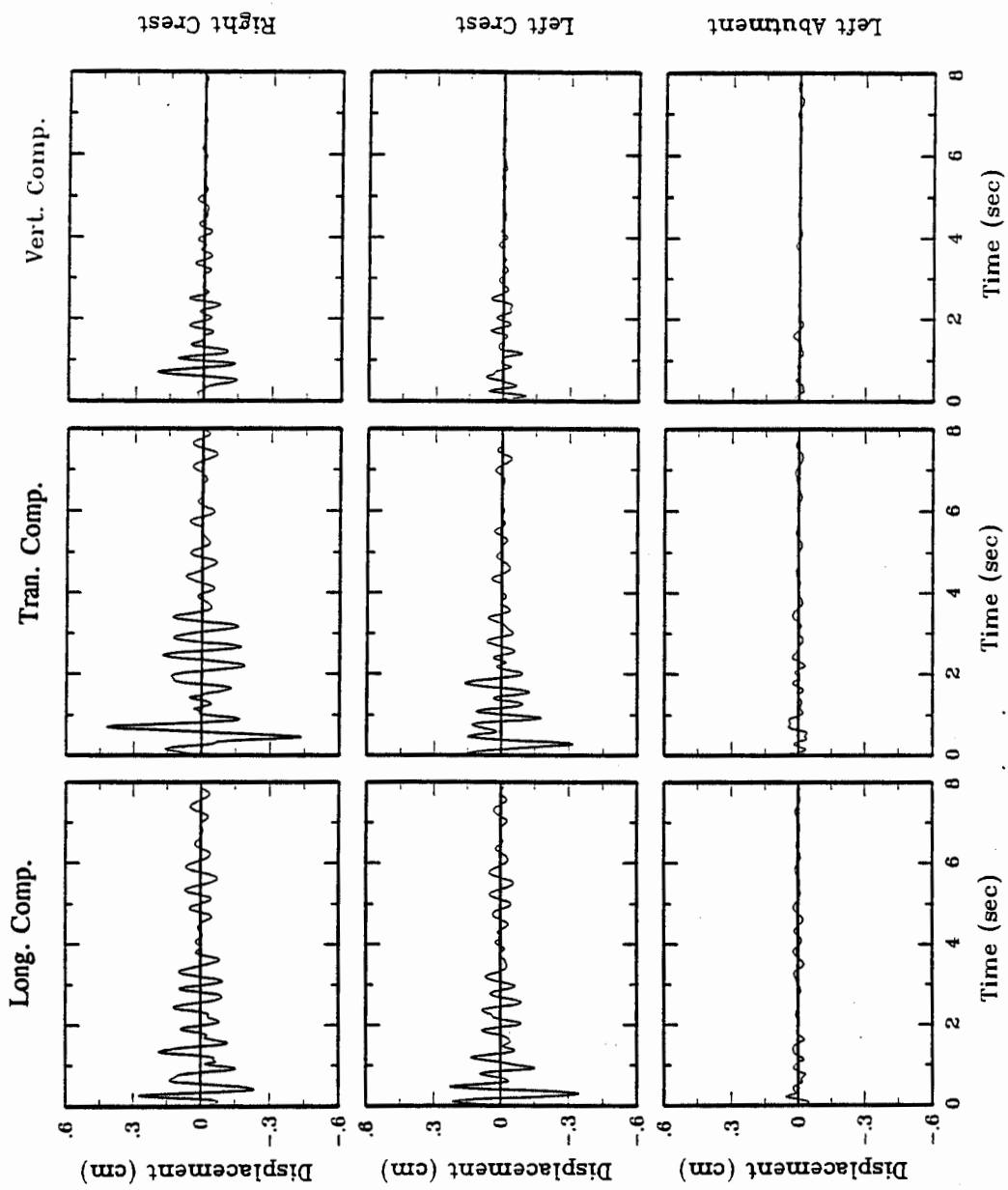


Figure 4(c): Displacement Time Histories Recorded at Lexington Dam During the Lake Elseman Earthquake of June 27, 1988

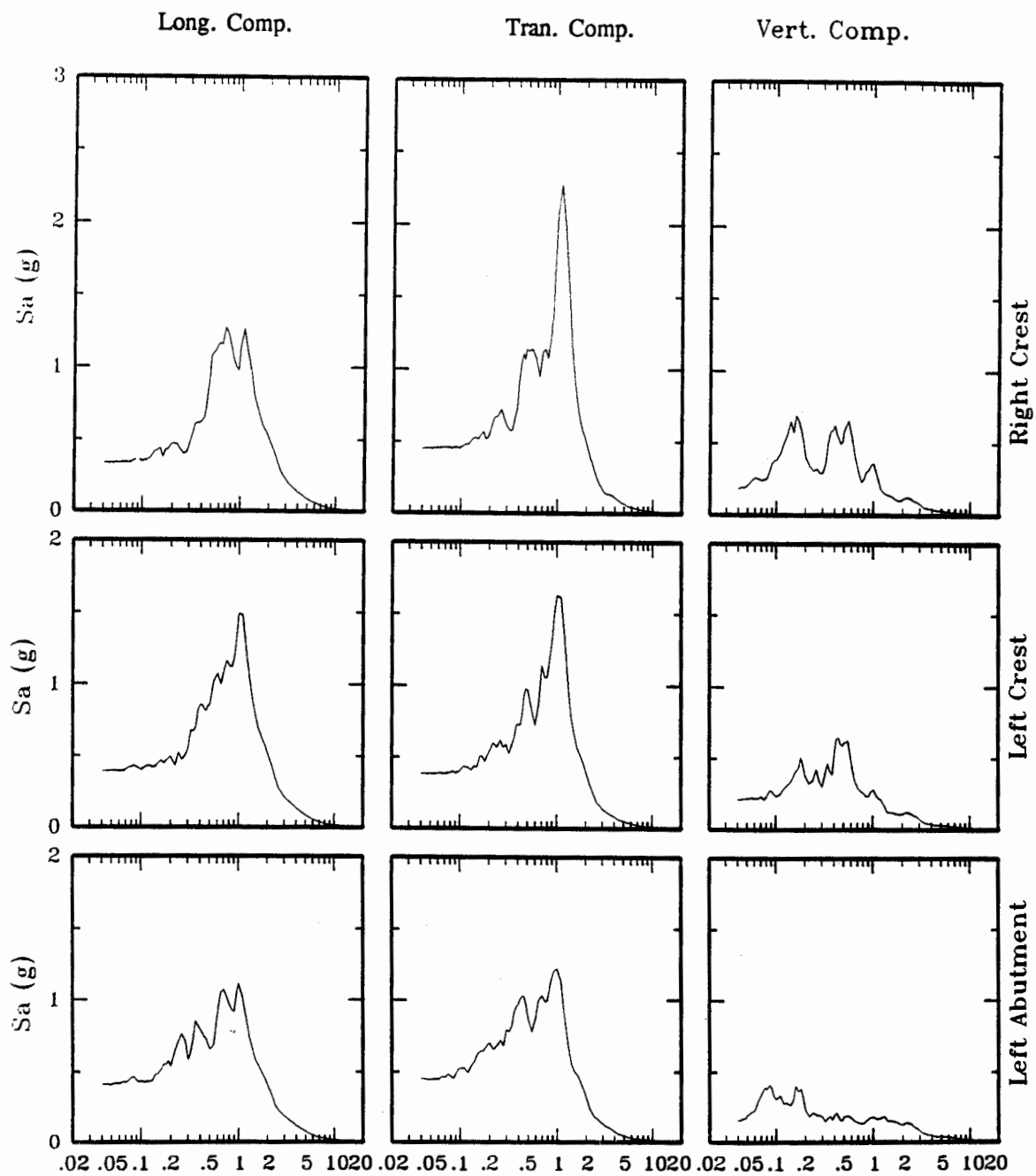


Figure 5(a): Acceleration Response Spectra (5% Damped) of Recordings at Lexington Dam During the Loma Prieta Earthquake of October 17, 1989

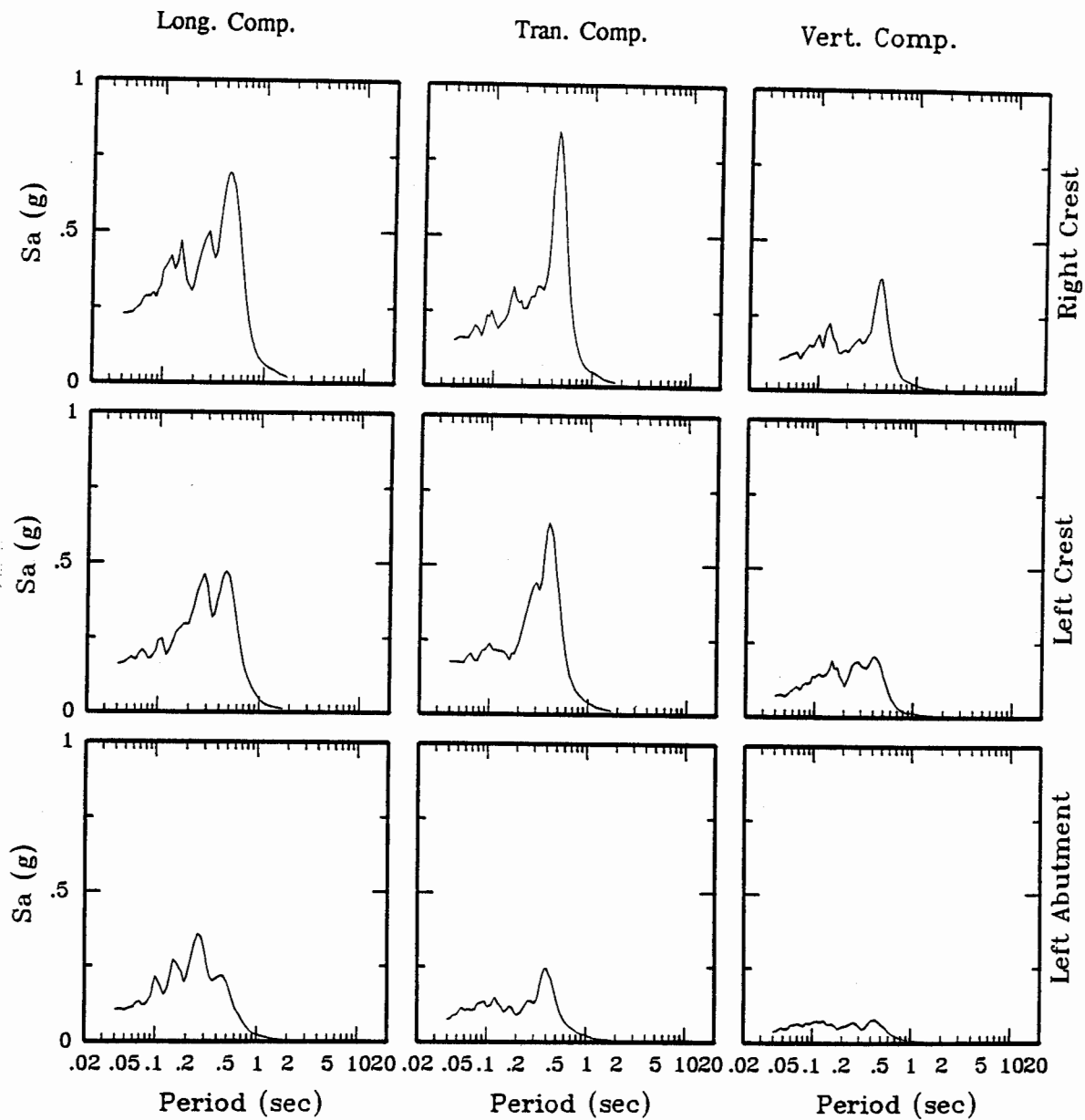


Figure 5(b): Acceleration Response Spectra (5% Damped) of Recordings at Lexington Dam During the Lake Elseman Earthquake of August 8, 1989

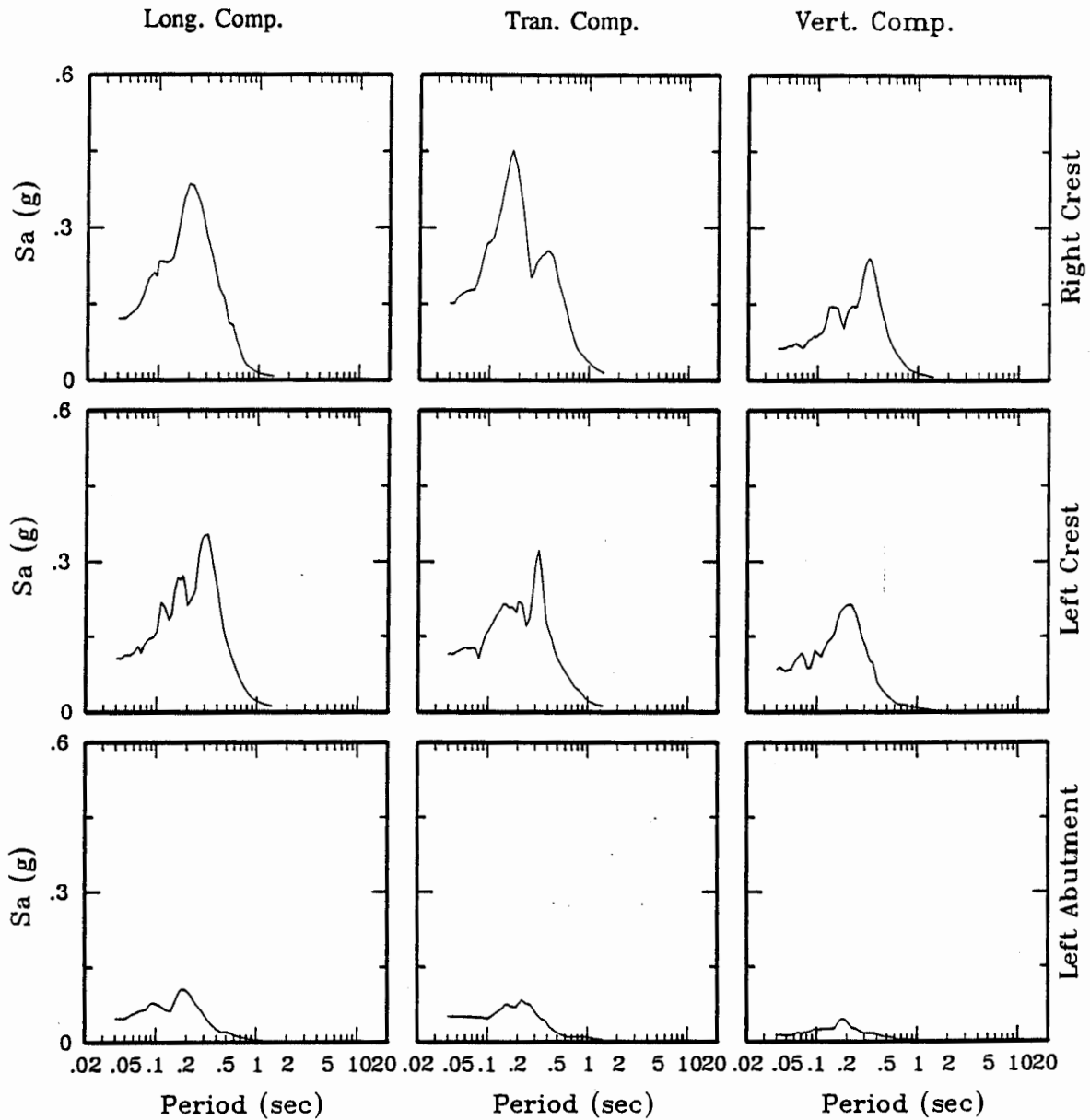


Figure 5(c): Acceleration Response Spectra (5% Damped) of Recordings at Lexington Dam During the Lake Elseman Earthquake of June 27, 1988

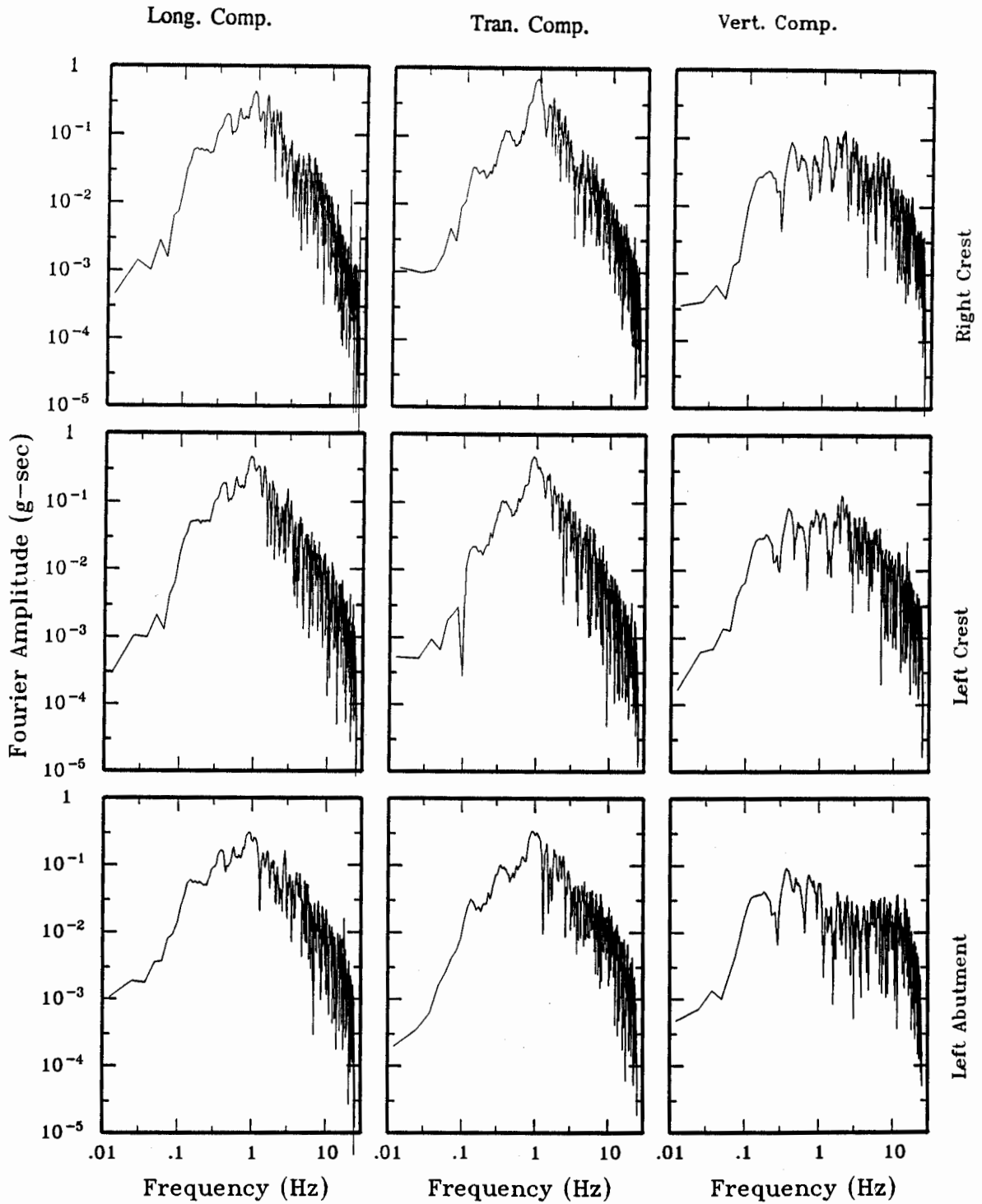


Figure 6(a): Fourier Amplitude Spectra of Recordings at Lexington Dam During the Loma Prieta Earthquake of October 17, 1989

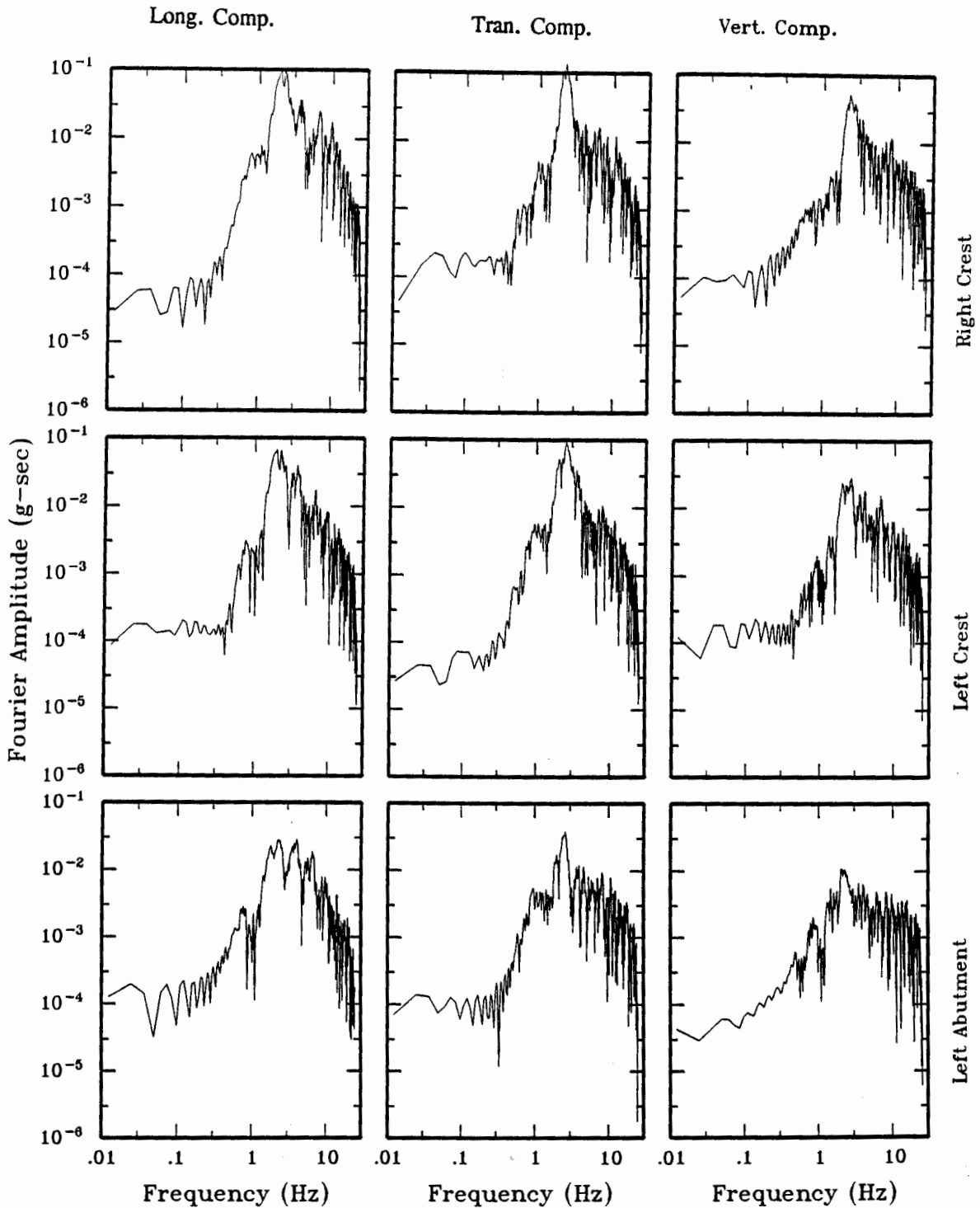


Figure 6(b): Fourier Amplitude Spectra of Recordings at Lexington Dam During the Lake Elsman Earthquake of August 8, 1989

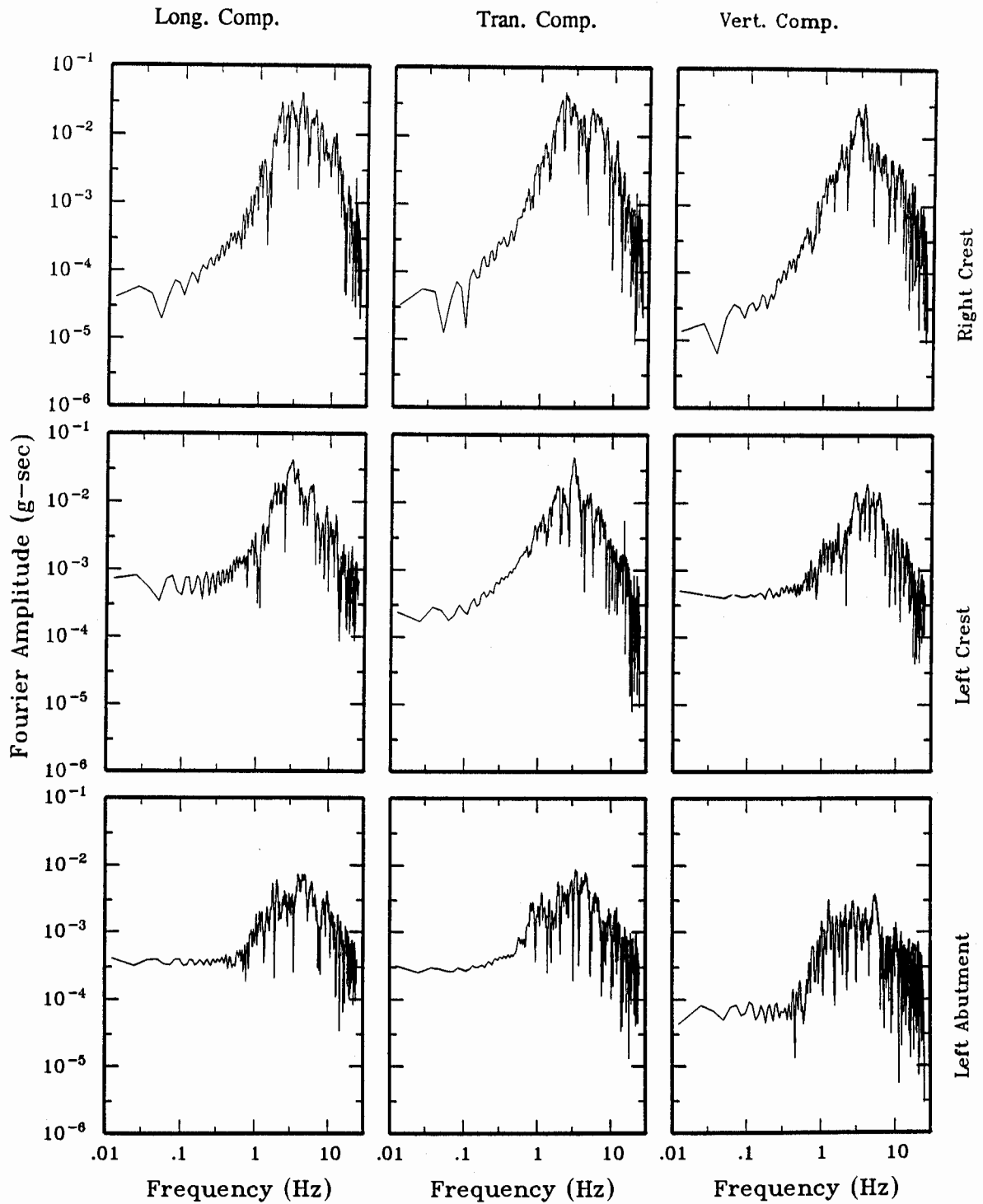


Figure 6(c): Fourier Amplitude Spectra of Recordings at Lexington Dam During the Lake Elsman Earthquake of June 27, 1988

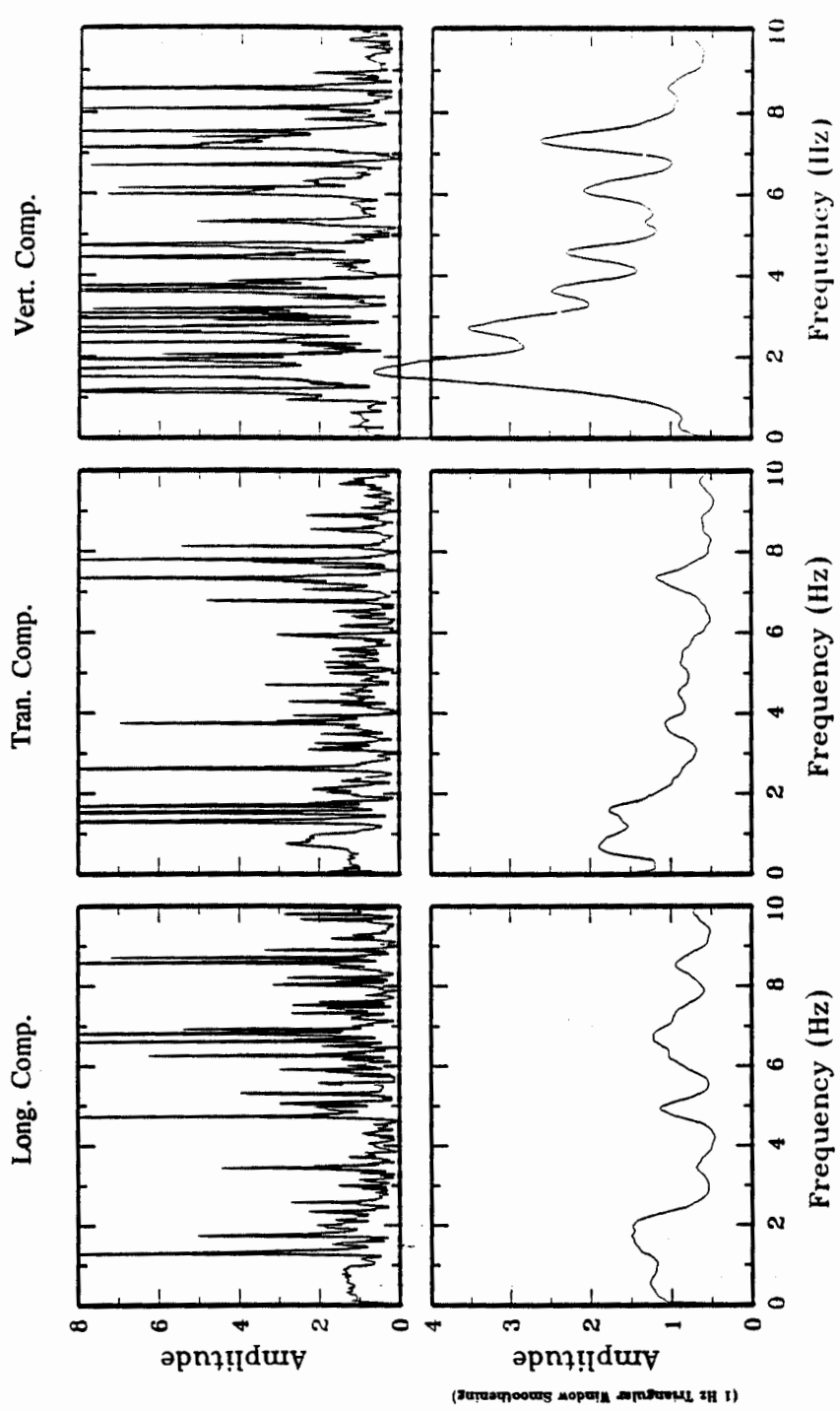


Figure 7(a): Fourier Amplitude Ratios (Right Crest/Left Abutment) of Recordings at Lexington Dam During the Loma Prieta Earthquake of October 17, 1989

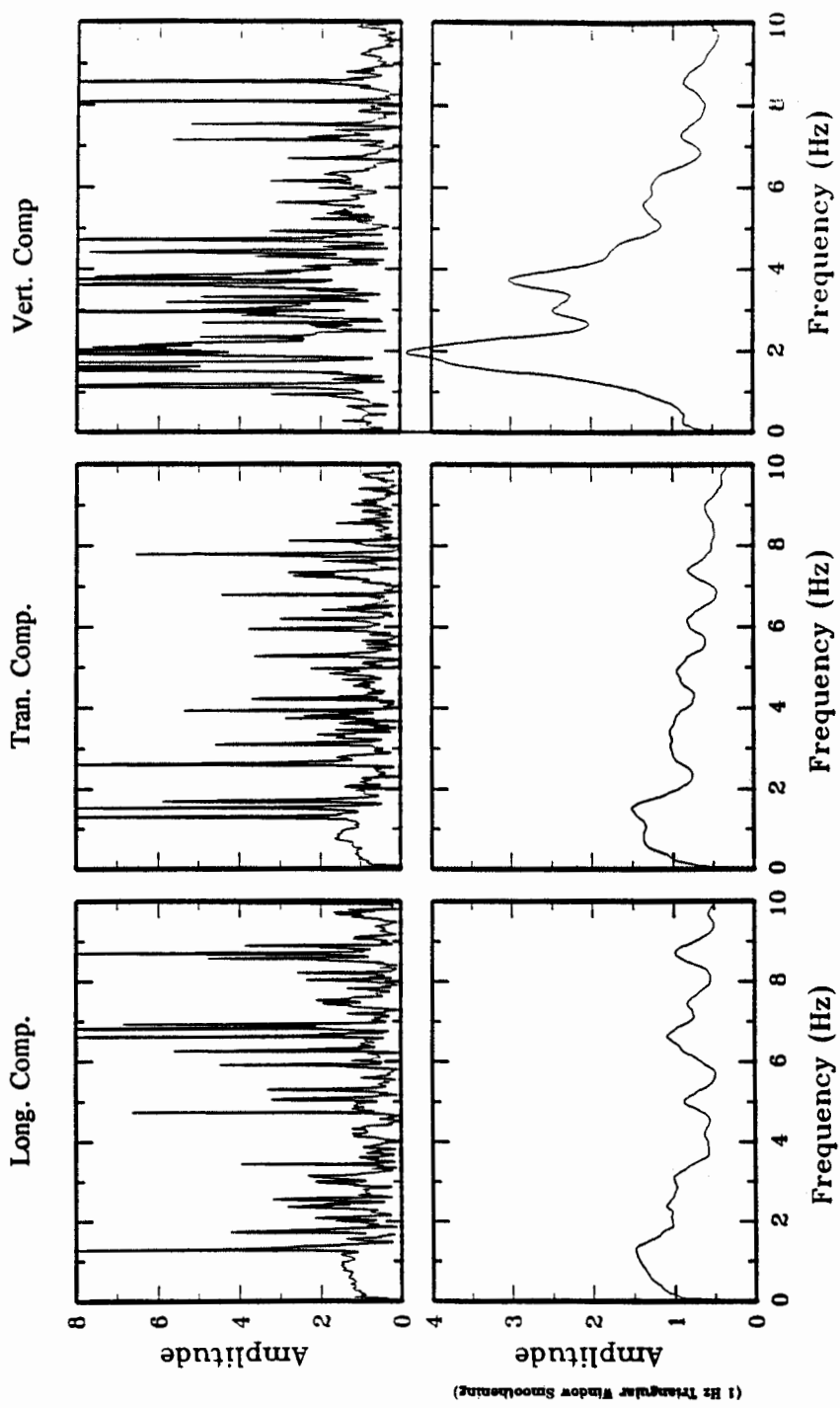


Figure 7(b): Fourier Amplitude Ratios (Left Crest/Left Abutment) of Recordings at Lexington Dam During the Loma Prieta Earthquake of October 17, 1989

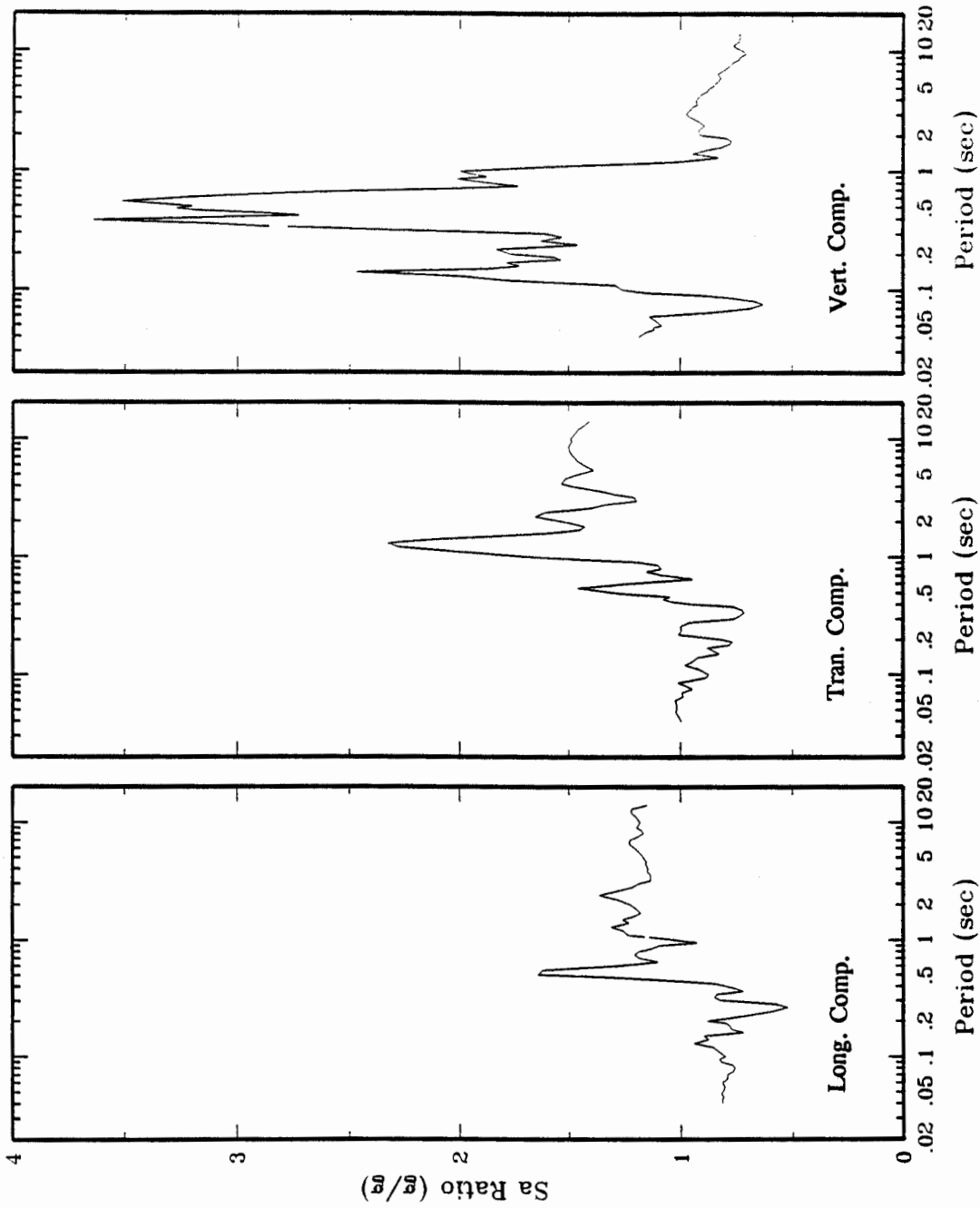


Figure 8(a) Response Spectral Ratios (Right Crest/Left Abutment) of Recordings at Lexington Dam During the Loma Prieta Earthquake of October 17, 1989

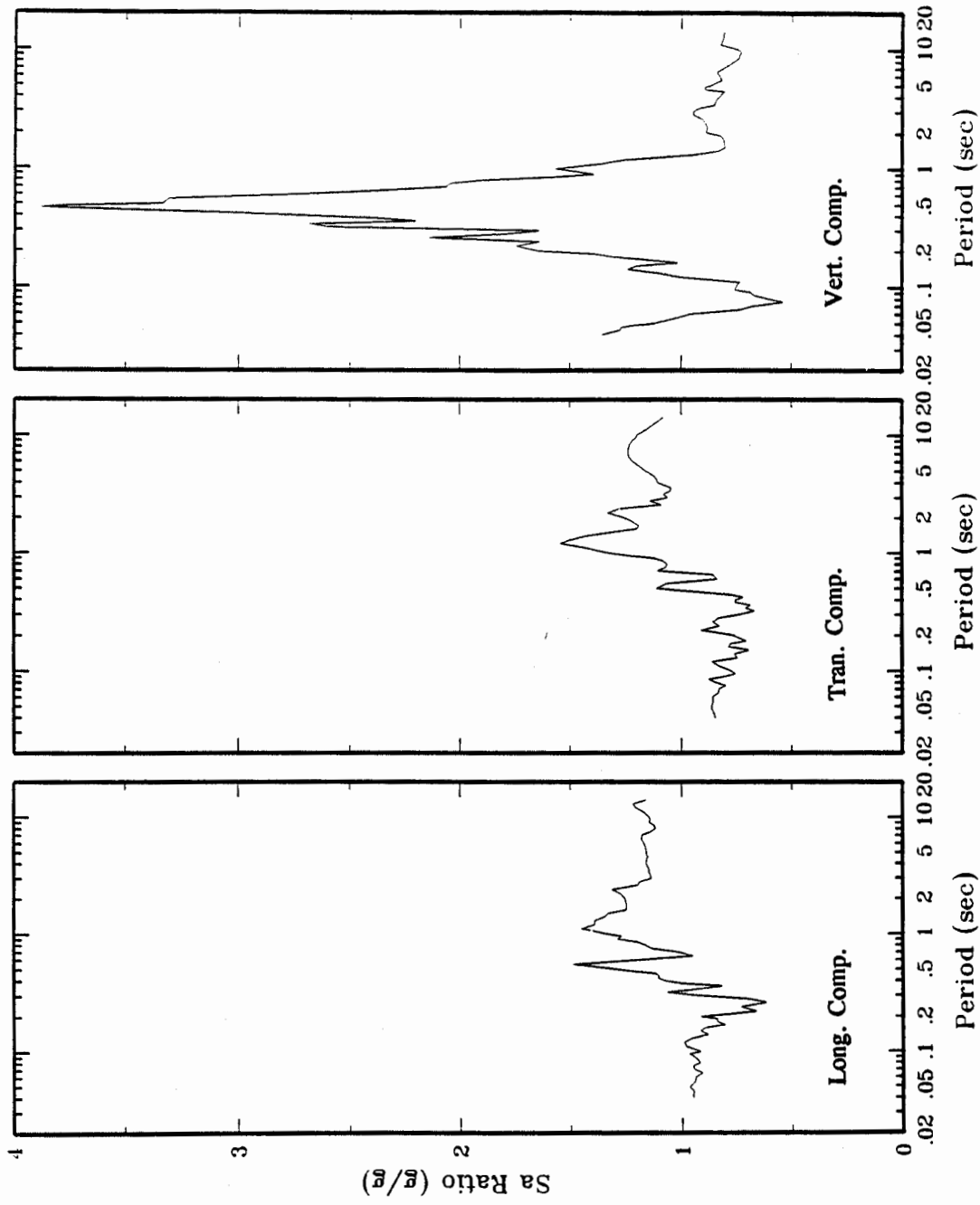


Figure 8(b): Response Spectral Ratios (Left Crest/Left Abutment) of Recordings at Lexington Dam During the Loma Prieta Earthquake of October 17, 1989

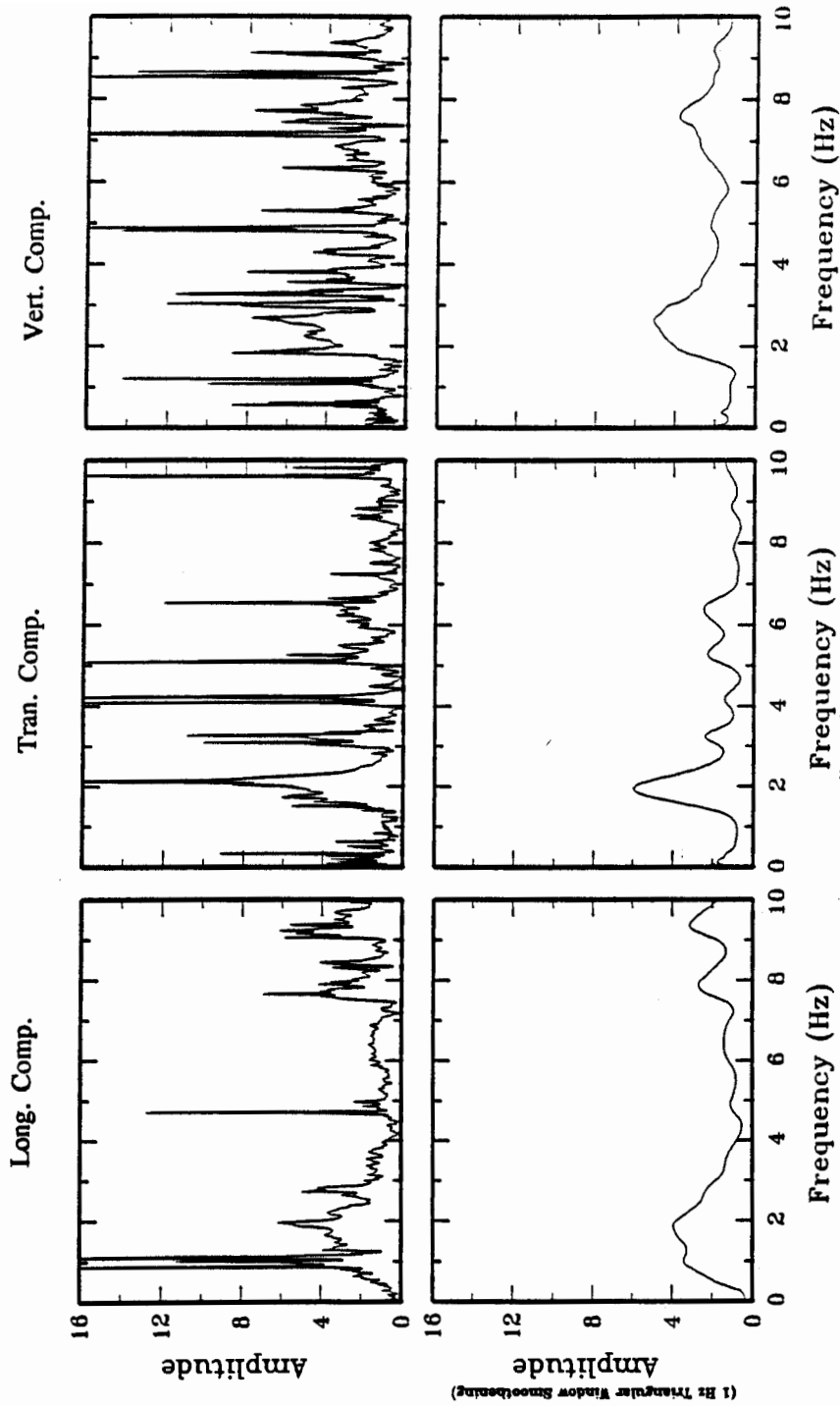


Figure 9(a): Fourier Amplitude Ratios (Right Crest/Left Abutment) of Recordings at Lexington Dam During the Lake Elseman Earthquake of August 8, 1989

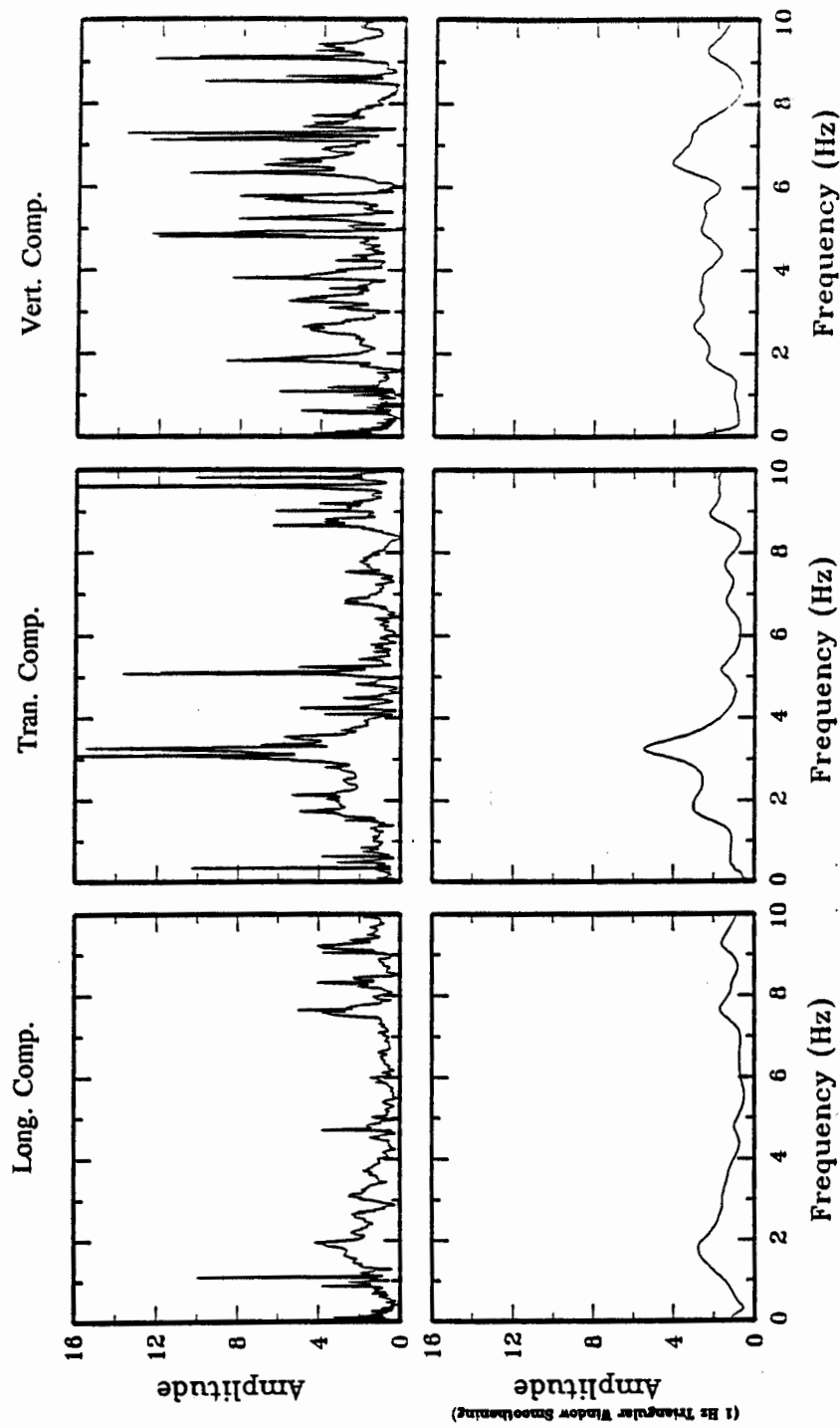


Figure 9(b): Fourier Amplitude Ratios (Left Crest/Left Abutment) of Recordings at Lexington Dam During the Lake Elseman Earthquake of August 8, 1989

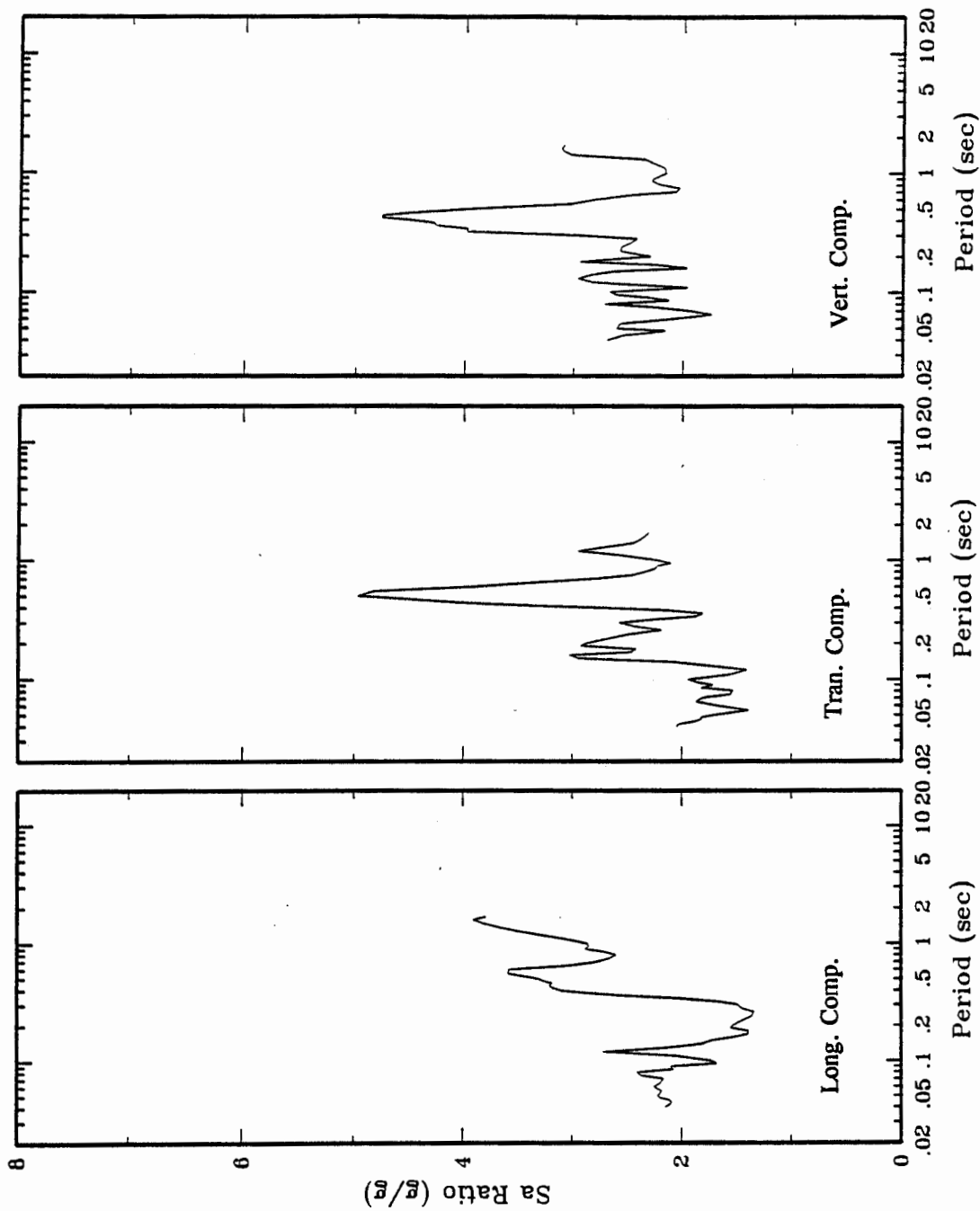


Figure 10(a): Response Spectral Ratios (Right Crest/Left Abutment) of Recordings at Lexington Dam During the Lake Elseman Earthquake of August 8, 1989

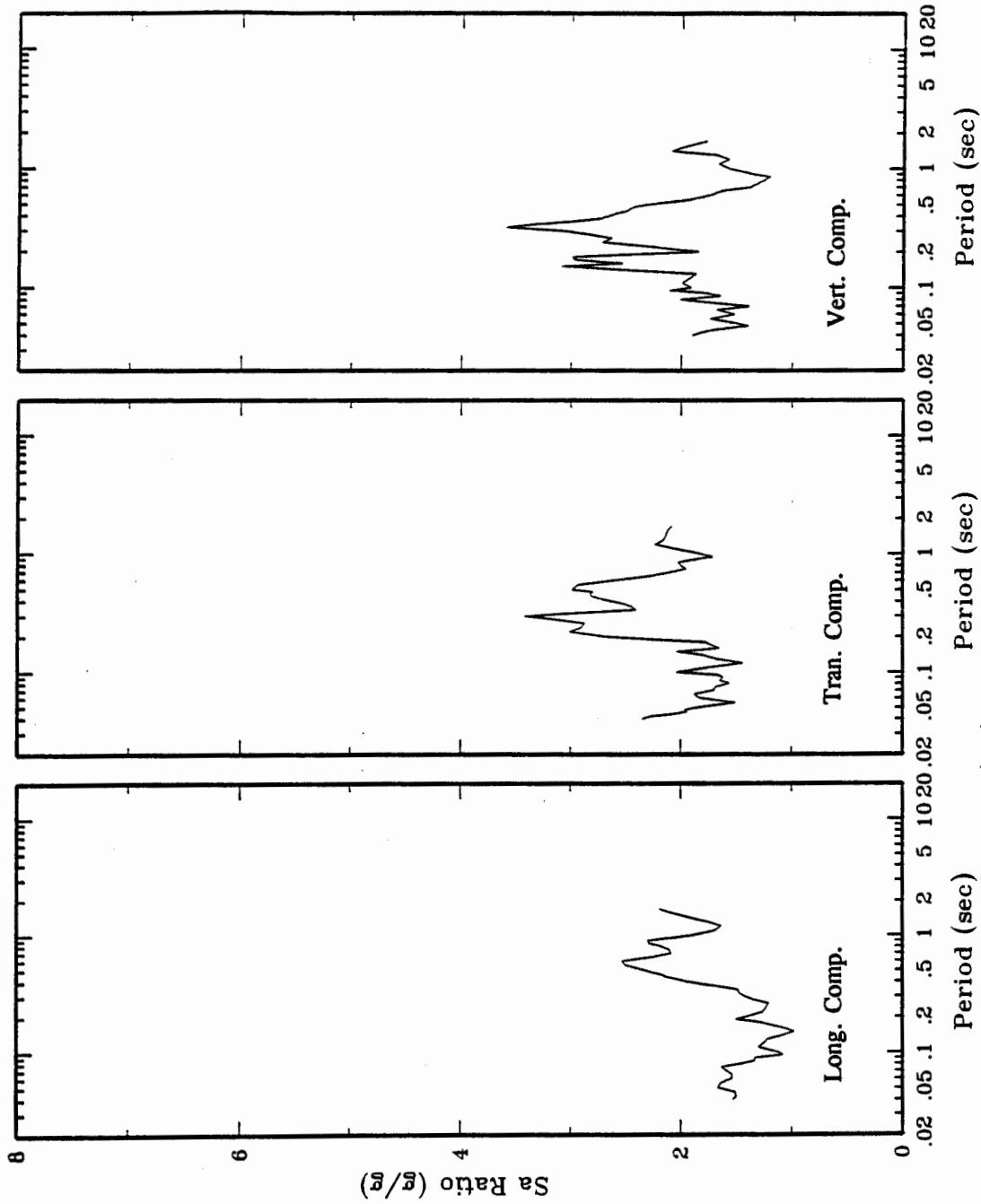


Figure 10(b): Response Spectral Ratios (Left Crest/Left Abutment) of Recordings at Lexington Dam During the Lake Elseman Earthquake of August 8, 1989

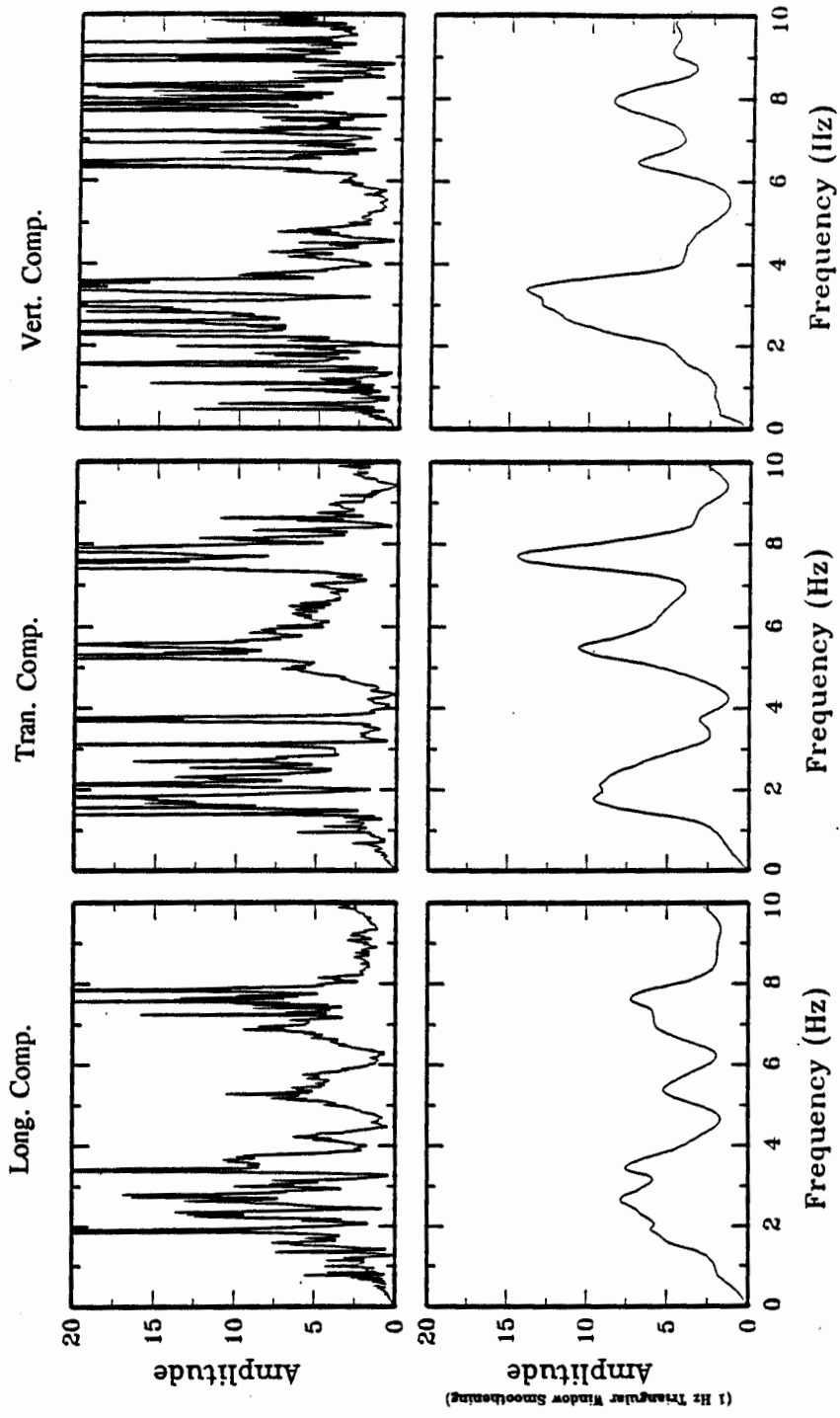


Figure 11(a): Fourier Amplitude Ratios (Right Crest/Left Abutment) of Recordings at Lexington Dam During the Lake Elseman Earthquake of June 27, 1988

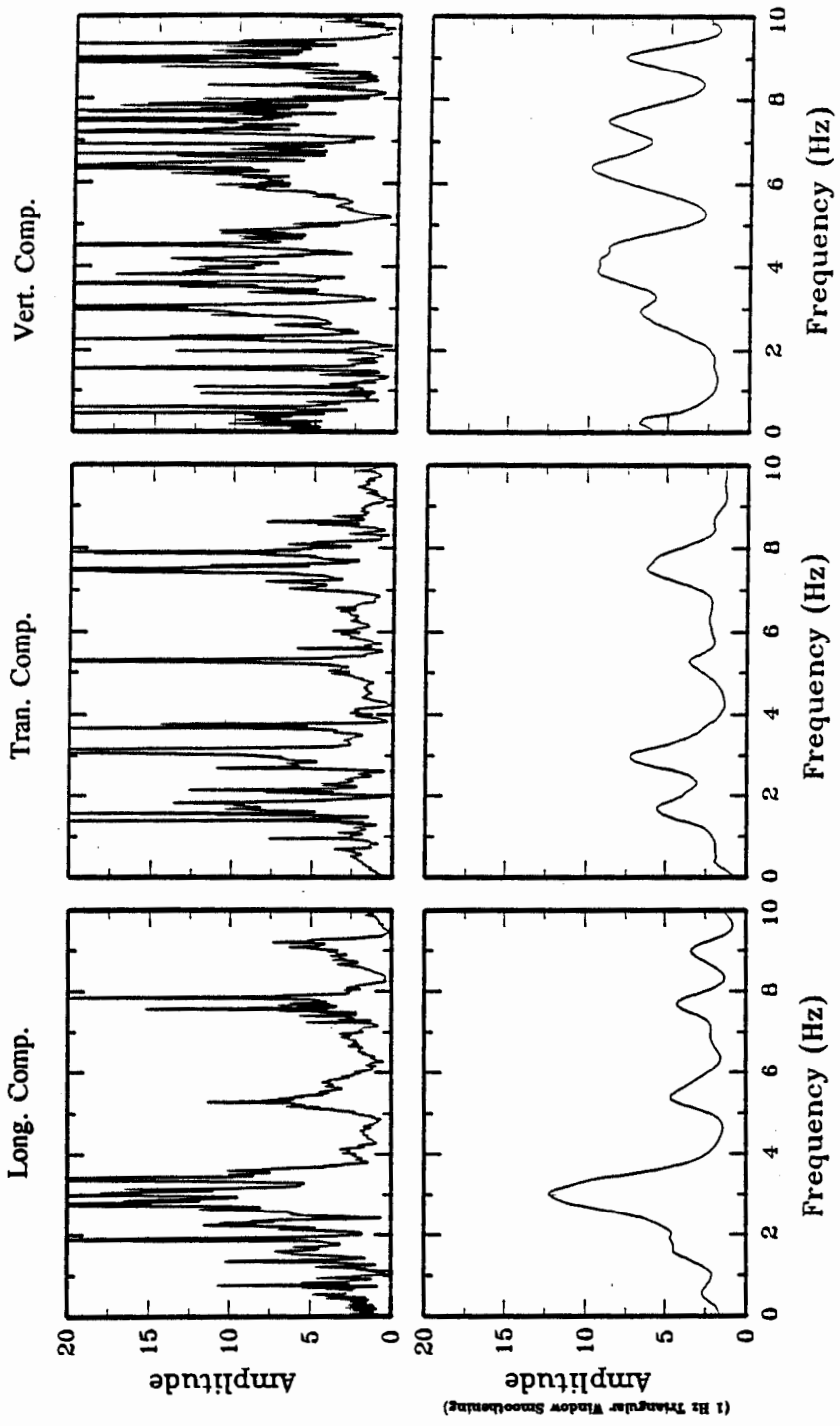


Figure 11(b): Fourier Amplitude Ratios (Left Crest/Left Abutment) of Recordings at Lexington Dam During the Lake Elseman Earthquake of June 27, 1988

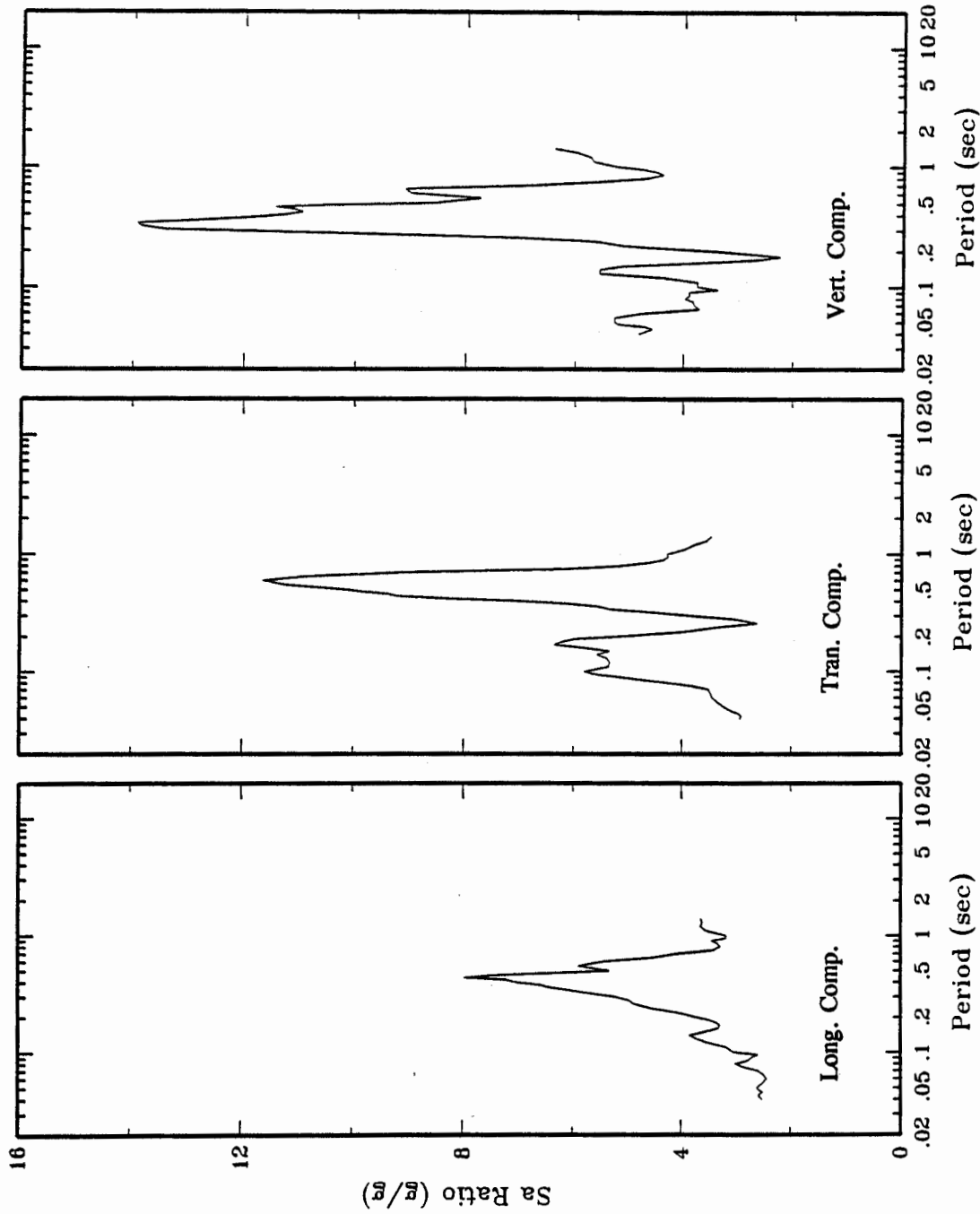


Figure 12(a): Response Spectral Ratios (Right Crest/Left Abutment) of Recordings at Lexington Dam During the Lake Elseman Earthquake of June 27, 1988

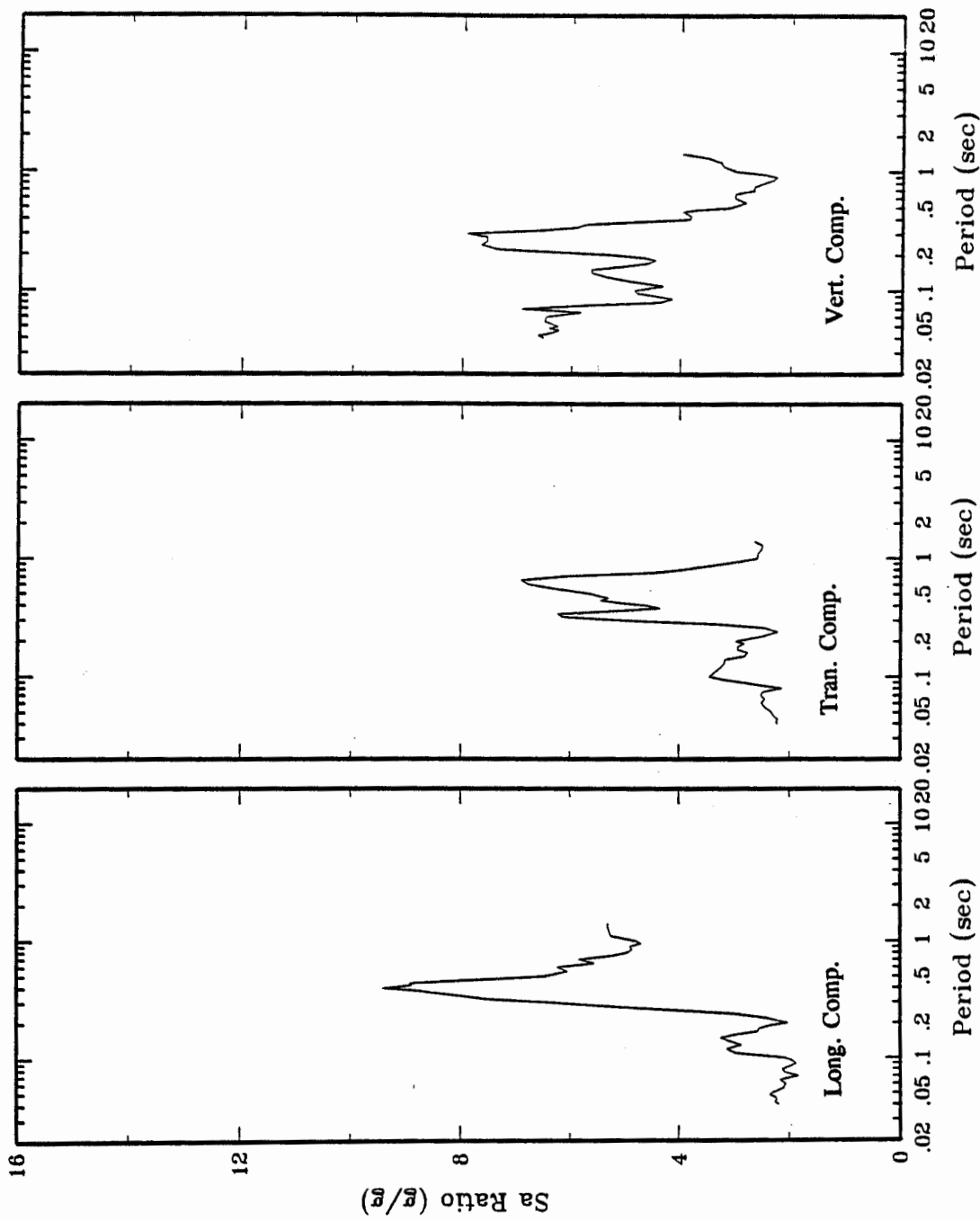


Figure 12(b): Response Spectral Ratios (Left Crest/Left Abutment) of Recordings at Lexington Dam During the Lake Elseman Earthquake of June 27, 1988

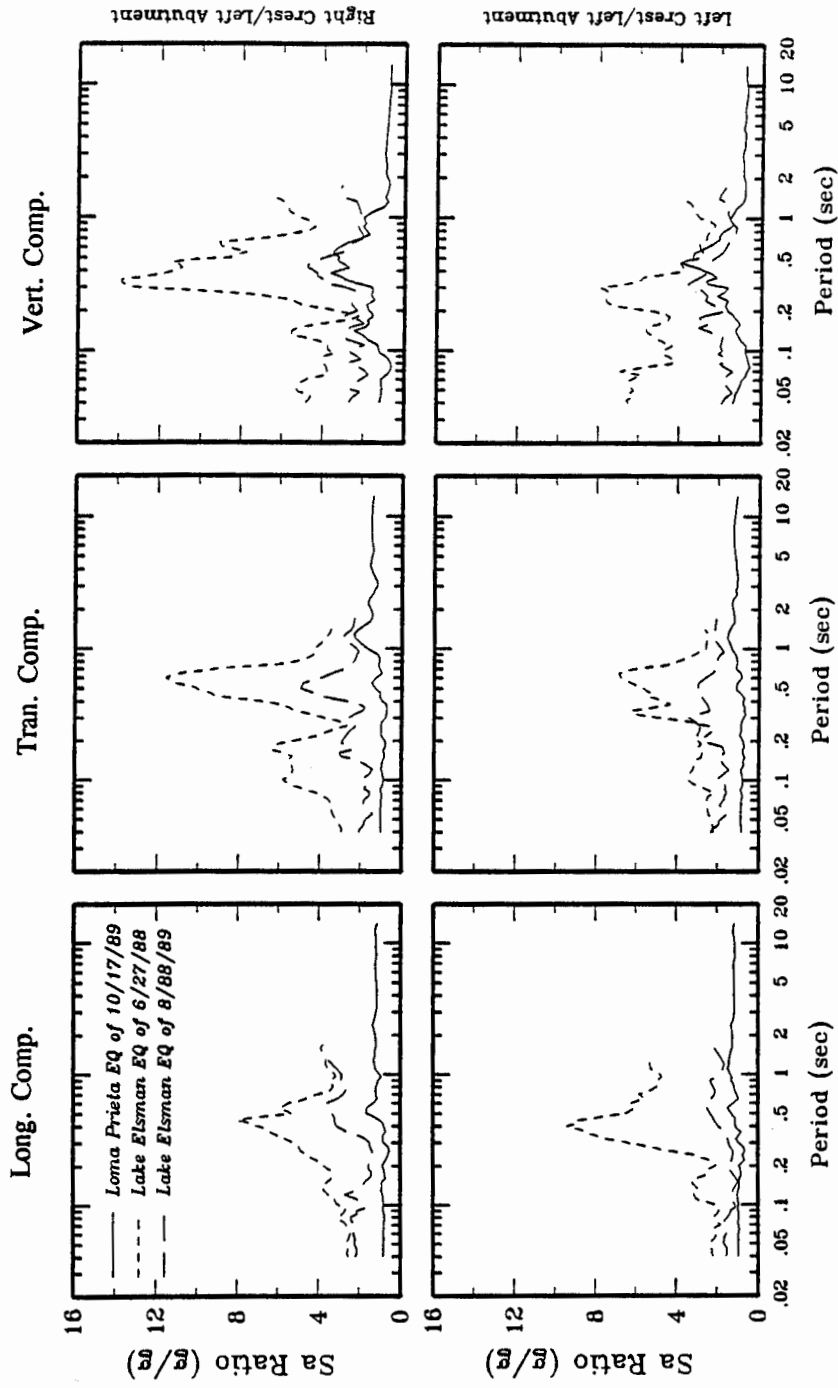


Figure 13: Summary Plots of Response Spectral Ratios (Crest to Abutment) at Lexington Dam for All Three Earthquakes

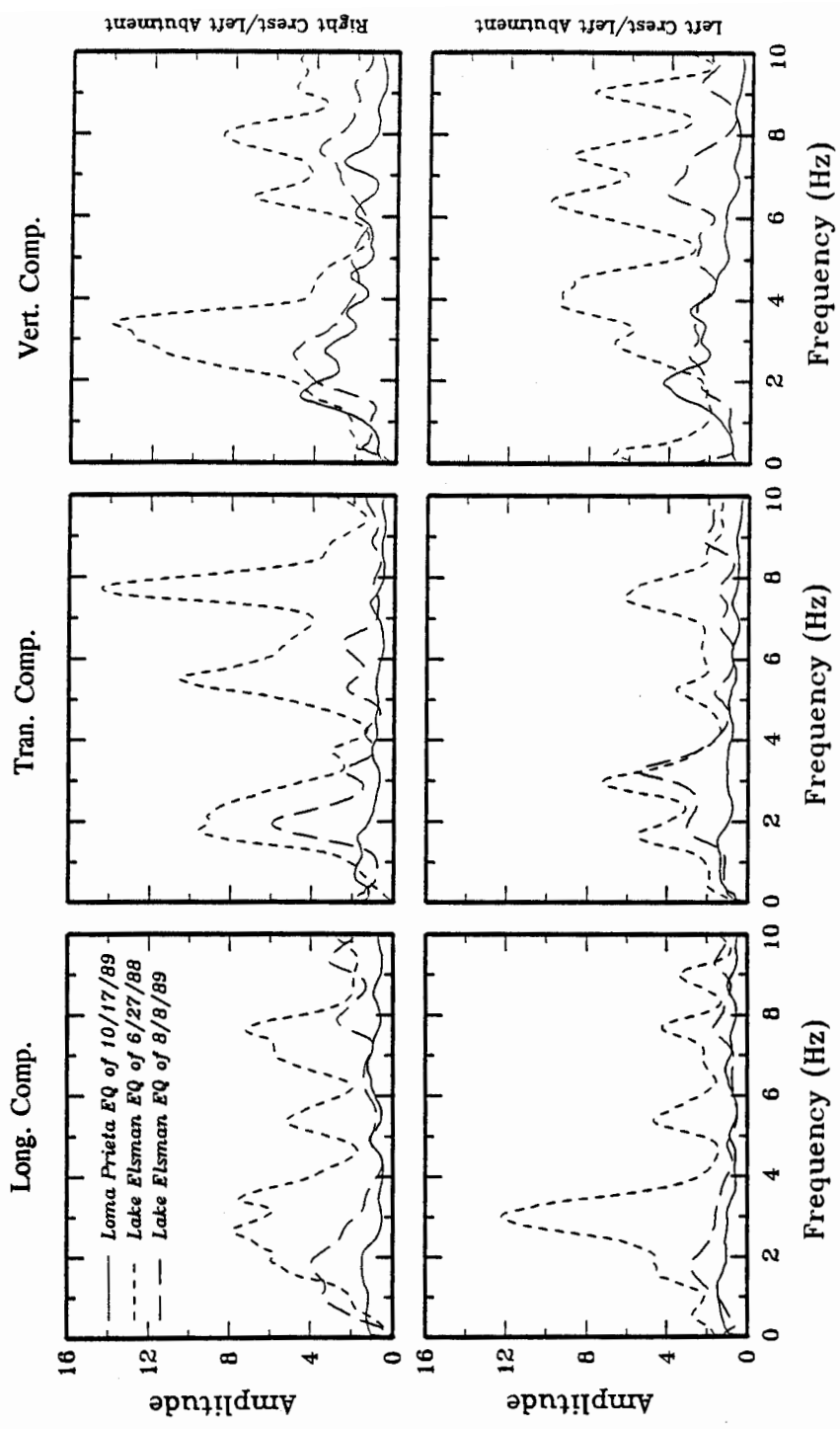


Figure 14: Summary Plots of Fourier Amplitude Ratios (Crest to Abutment) at Lexington Dam for All Three Earthquakes

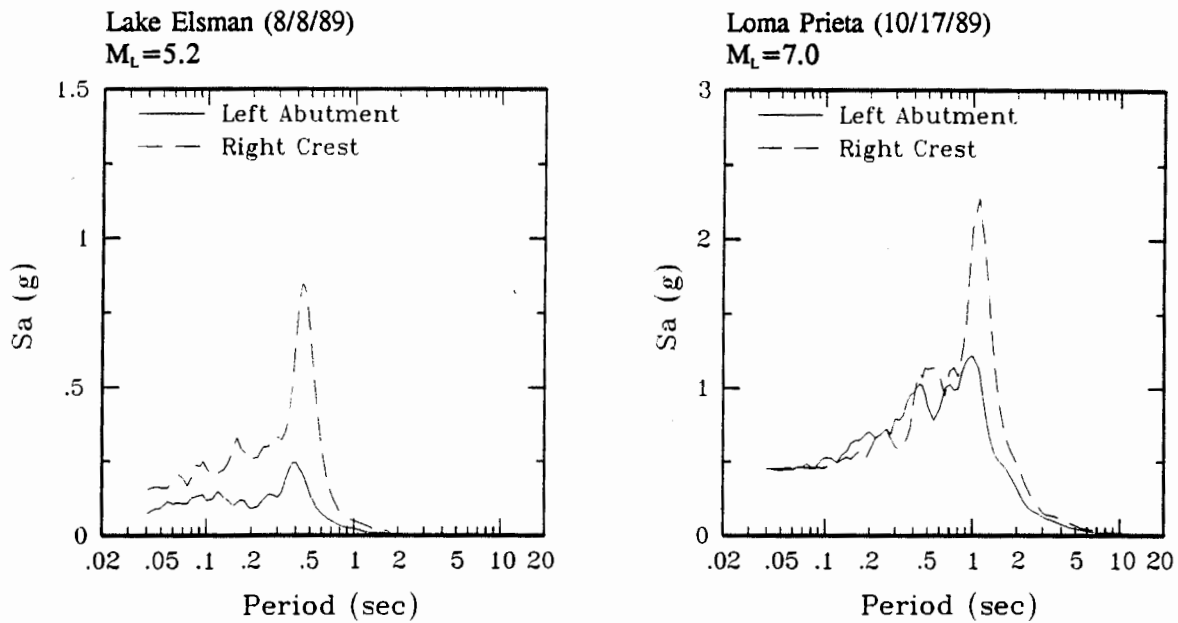


Figure 15: Response Spectra of Recorded Motions at Lexington Dam for the Two Events Used in the Response Analyses (Transverse Component, 5% Damping)

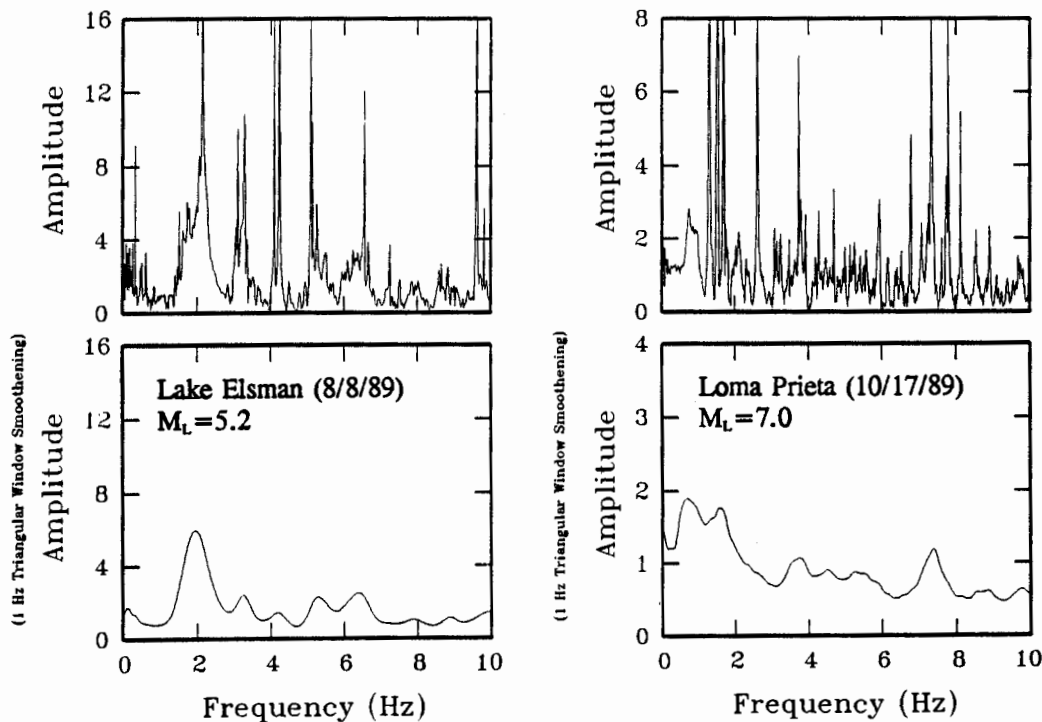


Figure 16: Fourier Spectral Ratios (Crest to Abutment) of Recordings at Lexington Dam for the Two Events Used in the Response Analyses (Transverse Component)

4 ANALYSES OF EMBANKMENT RESPONSE

To analyze the embankment response at the two levels of motion recorded during the Loma Prieta and Lake Elsmar earthquakes, we performed one- and two-dimensional dynamic finite element analyses. The analyses employed the method of complex response and an equivalent linear approximation of the strain-dependent modulus and damping properties of the embankment soils. The program SHAKE (Schnabel et al., 1972) was used for the one-dimensional wave propagation analyses, and FLUSH (Lysmer et al., 1975), a plane-strain, finite element analysis program, was used for the two-dimensional analyses. As mentioned earlier, all the analyses used the transverse component (component normal to the dam axis) of ground motion, and the cross section of the embankment used in the two-dimensional analyses was close to the right crest instrument.

4.1 TWO-DIMENSIONAL FINITE ELEMENT ANALYSES

Values of shear modulus at low strain (G_{max}) for various zones of the embankment and foundation were estimated on the basis of shear wave velocities measured in 1975 and 1981 (Wahler Associates, 1982). These values are summarized in Table 2.

TABLE 2
SHEAR WAVE VELOCITIES
USED IN RESPONSE ANALYSES OF LEXINGTON DAM*

Zone	Shear Wave Velocity (ft/sec)
All zones at shallow depth (0-20 ft)	1200
Lower core (below 80 ft depth)	1100 - 1500
Upper core and upstream shell	1400
Downstream shell (20-50 ft depth)	1700
Downstream shell (below 50 ft depth)	2200
Foundation rock	1800 - 3000

*Based on Wahler Associates, 1982

Wahler's geophysical field survey revealed shear wave velocities in the foundation bedrock that ranged from 1800 to 3000 ft/sec; average values in the shallow foundation were about 2200 ft/sec. Theoretical studies of dams that were located in canyons and had flexible rock foundations (Gazetas and Dakoulas, 1991) showed that when the ratio of canyon rock velocity to dam velocity was less than 10, assuming a rigid rock foundation changed the computed amplification function at the dam crest by more than 70% (see Figure 17). Accordingly, it was considered more appropriate to model the upper 300 to 350 ft of rock foundation as a flexible rock foundation and include it in the finite element mesh. Figure 18 shows the two-dimensional finite element representation of Lexington Dam and its flexible rock foundation. Horizontal transmitting boundaries were incorporated in the finite element idealization of the dam-foundation system. Shear wave velocities in the rock foundation were specified as follows: 0 to 100 ft depth: $v_s = 2500$ ft/sec; 100 to 200 ft: $v_s = 3000$ ft/sec; and 200 to 350 ft depth: $v_s = 4000$ ft/sec. This distribution of shear wave velocities was based on data from similar sites underlain by Franciscan rock formations where shear wave velocities have been measured with depth. The transverse component of rock motion recorded at the left abutment outcrop was used as input to the finite element analyses and was specified as surface motion of a free-field rock column. A schematic showing the location of the specified input motion appears as Figure 19. Use of this input motion implies that rock motions at the left abutment and at the valley floor (at the level of the base of the embankment) are similar. This assumption was verified by one-dimensional wave propagation studies as well as by results of the two-dimensional finite element and finite difference studies of topographic effects on similar slopes at the Diablo Canyon site (Pacific Gas and Electric Co., 1988). Two factors affect the computed response at the crest of the embankment for a specified set of shear wave velocities: (a) the variation of shear modulus and damping with strain of the embankment materials; and (b) the depth to the rigid rock foundation. Our analyses considered both these factors, the effects of which are summarized below.

4.1.1 Effects of Modulus and Damping Relationships

Relationships that describe the variation of modulus and damping properties with strain were obtained from published literature concerning similar soils: Seed and Idriss (1970) and Seed et al. (1984) for cohesionless soils; and Sun et al. (1988) for cohesive soil. These relationships are shown on Figure 20. The Sun et al. (1988) modulus curve is for cohesive soils having plasticity index values of 20 to 40. The finite element section with the shear wave velocities shown on Figure 18 was analyzed using the modulus and damping relationships shown on Figure 20. We used the two-dimensional dynamic finite element analysis program FLUSH, with the rigid rock foundation assumed to be 350 ft below ground surface. We made parametric studies to evaluate the effects on the predicted response of using various modulus reduction and damping curves. The modulus and damping relationships that produced a computed response that best matched the recorded response (for both events) were the mid-range shear modulus reduction curve proposed by Seed and Idriss (1970) for sands and their lower-bound damping curve. As described earlier, the lower core zone (below a depth of 80 ft) was more cohesive, having 85% fines of medium to high plasticity. Accordingly, one additional case was analyzed using both these curves and the modulus reduction curve proposed by Sun et al. (1988) for the lower core zone. The results of these analyses are presented on Figure 21 in terms of 5% damped acceleration response spectra at the crest of the dam, compared to the spectra recorded at the right crest location. Figure 21(a) shows the computed and recorded response at the crest of the dam for the Lake Elsmar event of August 8, 1989; Figure 21(b) shows the corresponding results for the Loma Prieta event. These results show that the mid-range modulus curve and the lower-bound damping curve proposed by Seed and Idriss (1970) provided results that are in better agreement with the recorded response. These relationships, presented in Table 3, were used in the analyses presented herein. Figure 22 shows a comparison between the computed and recorded acceleration time-histories at the crest of the embankment using the modulus and damping relationships shown in Table 3.

TABLE 3
MODULUS REDUCTION AND DAMPING CURVES
USED IN ANALYSES*

Shear Strain (%)	G/G_{max}	Damping Ratio
10^{-4}	1.0	0.3
10^{-3}	0.97	0.8
10^{-2}	0.73	2.8
10^{-1}	0.30	10.0
1	0.05	21.0

*From Seed & Idriss, 1970

4.1.2 Effect of Depth to Rigid Boundary

The results shown on Figure 21 were obtained for the finite element mesh of Figure 18, assuming a flexible rock foundation that extends to about 350 ft below ground surface. To evaluate the effect of the location of the rigid boundary on the computed response at the crest of the dam, three additional cases were analyzed. The first case involved extending the flexible rock foundation to 600 ft and placing the rigid boundary at that depth. In the second, the program SuperFlush (Udaka, 1989) was used to place a half-space at a depth of 350 ft. SuperFlush provides a capability of placing a compliant flexible half-space at the foundation level. This option is not available in the program FLUSH which only allows for a rigid base at the foundation. In the third case, the foundation bedrock was assumed to be rigid; thus the rigid boundary was placed at the base of the embankment. The results of the analyses for these cases, in terms of 5% damped response spectra at the crest of the dam, are shown on Figure 23. The results on Figure 23(a) for the Lake Elsmann event show that placing the rigid boundary at 350 ft or 600 ft, or using a half-space analysis, did not change significantly the computed spectra at the crest of the dam. However, placing the rigid boundary at the base of the embankment did change the computed spectrum at the crest of the embankment significantly from those obtained for the flexible rock foundation. This observation is consistent with the results shown on Figure 17. Because the

finite element analyses showed that (at the low level of shaking of the Lake Elsmar event) the ratio of foundation (canyon) shear wave velocity to that of the embankment was about 2.5, it is unreasonable to assume a rigid rock foundation at the base of the embankment. It is interesting to note that the computed response, for the case where the rigid boundary was at the base of the dam, showed the best fit to the recorded response. However, such good agreement is fortuitous. The results for the Loma Prieta event, presented on Figure 23(b), show that the computed response at the crest is not sensitive to the location of the rigid boundary. The conclusion is not unexpected: at the high level of shaking of the Loma Prieta earthquake, the embankment modulus (and thus shear wave velocity) was reduced sufficiently that the ratio of the foundation bedrock velocity to that of the embankment increased about eightfold. Thus the assumption of rigid rock at the base of the embankment becomes a reasonable approximation. In any case, for all the analyses described below, the rigid boundary was kept at 350 ft below the surface, as shown in the finite element section of Figure 18.

The results of the two-dimensional finite element analyses for both events, for the embankment section and properties shown on Figure 18 and for the modulus and damping relationships given on Table 3, are presented on Figure 24 in terms of the computed and recorded 5% damped acceleration response spectra at the crest of the dam. There is reasonable agreement between the computed and recorded spectra for the Loma Prieta event at periods of 0.2 seconds and longer, although the peak ground acceleration is over-predicted by as much as 45%. For the Lake Elsmar event, although the computed prediction approximates the first natural period of the embankment, the predicted spectral accelerations are about 60% of the recorded ones at periods less than 0.5 seconds. Possible reasons for the discrepancies between the computed and recorded ground motions may be related to: (a) the assumption of vertically propagating shear waves used in the analyses; (b) three-dimensional effects of the triangular-shaped canyon; and (c) possible

interaction between the dam and its abutment and its effect on ground motions recorded at the left abutment instrument.

Figure 25 shows the computed Fourier amplitude transfer functions between the dam crest and left abutment recordings for both events analyzed. Again there is reasonable agreement between the computed transfer functions shown on Figure 25 and those obtained from the recorded motions shown on Figure 16. The first natural periods of the embankment computed using the finite element analysis are about 0.55 seconds for the smaller Lake Elsmar event and about 1.3 seconds for the Loma Prieta event.

The shift in the fundamental natural period of the embankment with increased level of ground shaking reflects the strain-dependent, nonlinear behavior of the embankment soils. This is demonstrated on Figure 26 as a plot of the G/G_{\max} and damping values vs. shear strain for elements at the centerline of the dam extending between the crest and the foundation. This plot shows that, for the Lake Elsmar earthquake, the strain levels were about 0.004% to 0.03%, with a corresponding reduction in G_{\max} of about 20% to 40%. This is in contrast with the Loma Prieta event, where the developed strain level ranged from about 0.1% to 1.0%, with a corresponding reduction in shear modulus of about 60% to 95% of the initial low strain value.

4.2 ONE-DIMENSIONAL ANALYSES

The response of the embankment was also computed using one-dimensional wave propagation analysis with the program SHAKE. The purpose of this exercise was to evaluate the validity of using the one-dimensional approximation in predicting the two-dimensional embankment response. Our analysis assumed a one-dimensional soil column representing the height of the embankment and the material properties below the crest. The input base motion used was the transverse component of the left abutment recording (as with the two-dimensional finite element analysis), and the rock foundation was assumed to be rigid below the base of the embankment. The results of this analysis

for both events are shown on Figure 27 in terms of recorded and computed 5% damped acceleration response spectra at the crest of the embankment. This figure also shows the results for the corresponding case of the two-dimensional finite element analyses. This figure shows that results of the one-dimensional approximation are in poor agreement with the recorded ground motions at the crest and with those obtained from two-dimensional analyses. Computed peak ground accelerations at various depths below the crest from one-dimensional analyses were about 30% to 50% of those computed from the two-dimensional analyses. Values of the computed maximum shear stresses and shear strains were lower than the corresponding two-dimensional values by about the same margins.

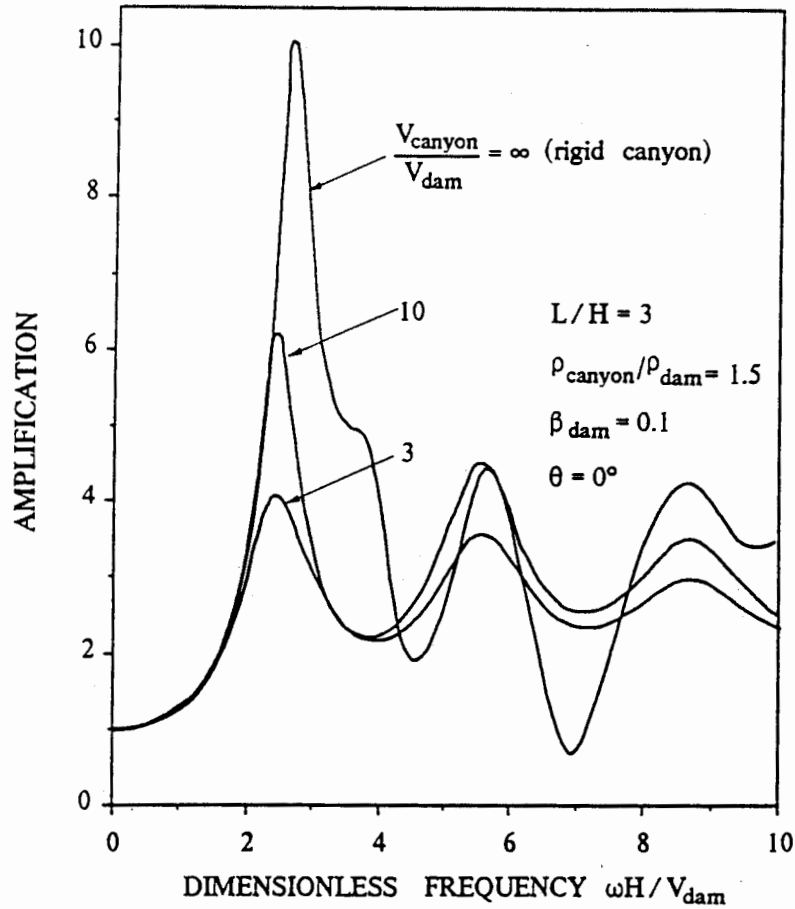
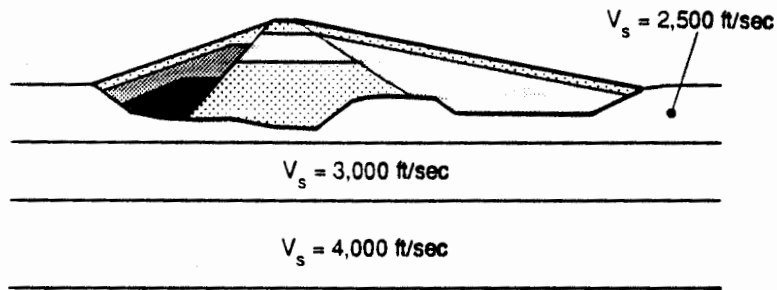


Figure 17: Mid-Crest Amplification Versus Dimensionless Frequency for Three Dams With S-Wave Velocity Ratios $V_{\text{CANYON}}/V_{\text{DAM}} = 3, 10,$ and ∞ (Rigid Canyon) in Rectangular Canyons Subjected to Vertically Propagating SH Waves (from Gazetas and Dakoulas, 1991)



EXPLANATION

	$V_s = 1,200$ ft/sec		$V_s = 1,700$ ft/sec
	$V_s = 1,400$ ft/sec		$V_s = 2,200$ ft/sec

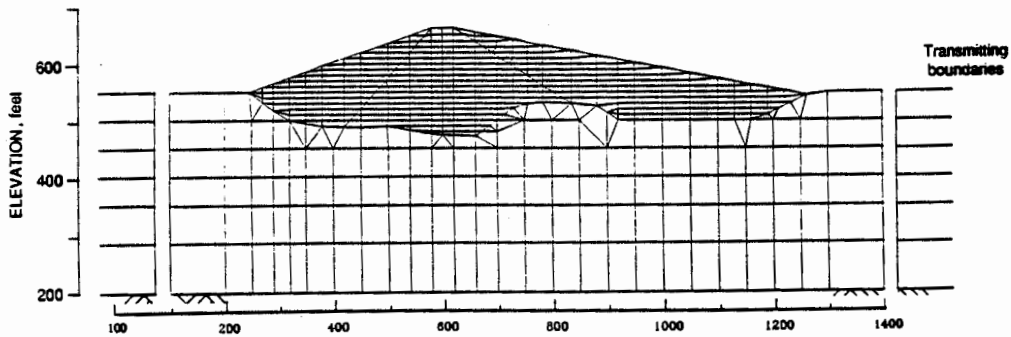


Figure 18: Finite Element Representation and Shear Wave Velocities of Lexington Dam and Its Foundation

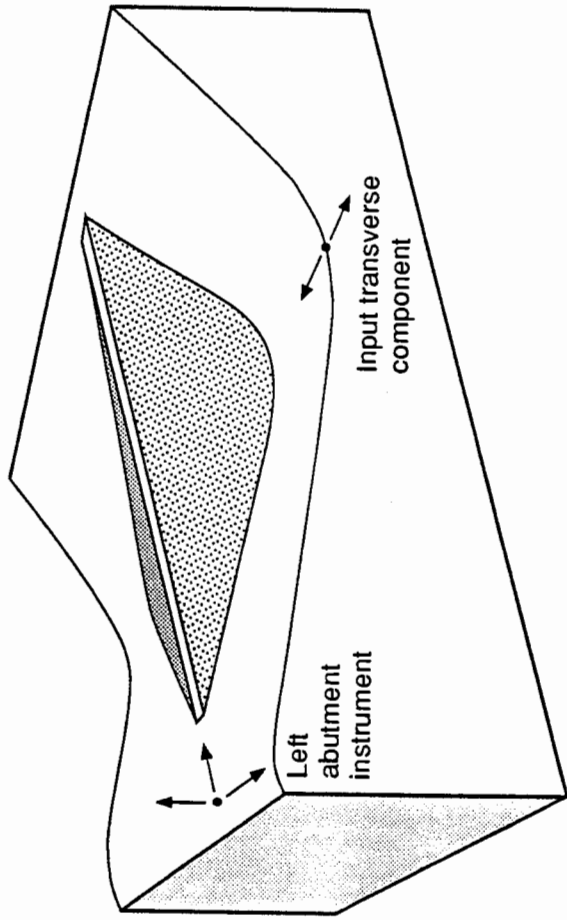


Figure 19: Schematic Representation of Input Motion for the Lexington Dam Analyses

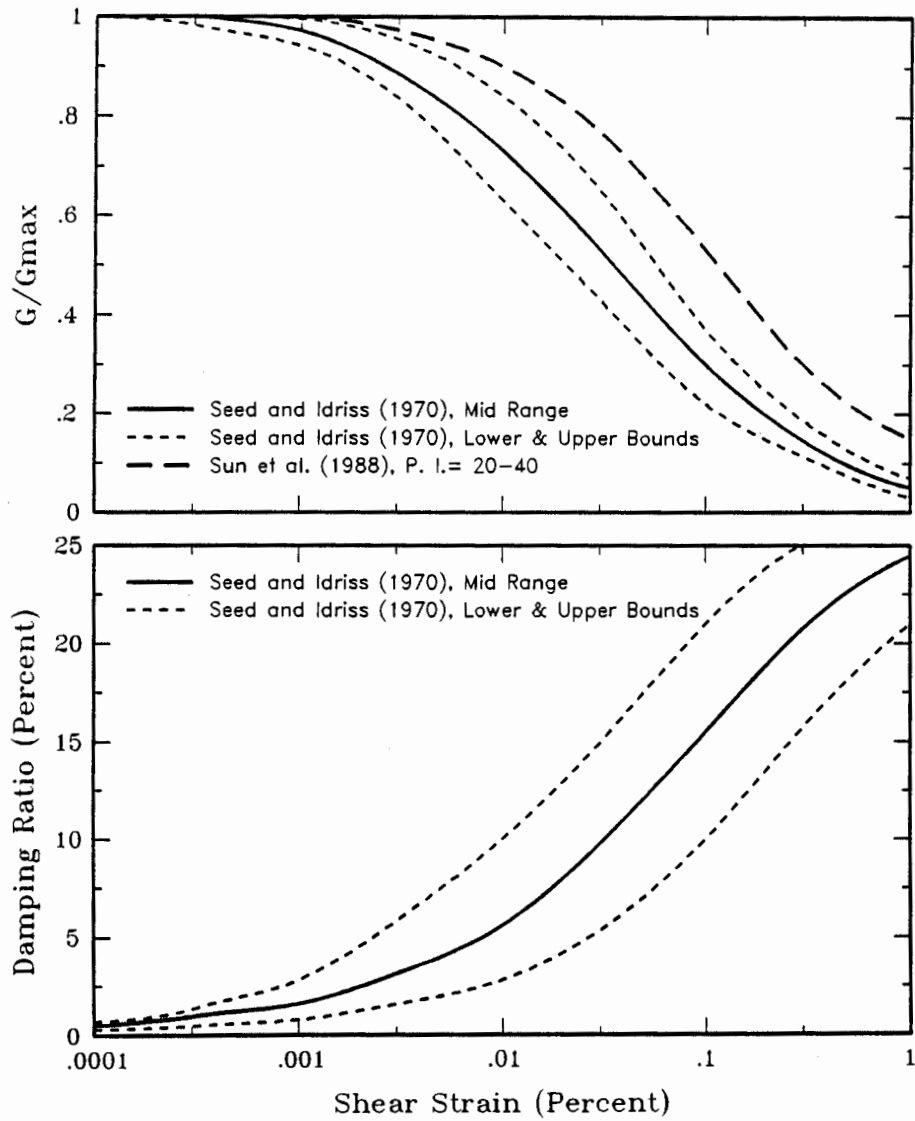
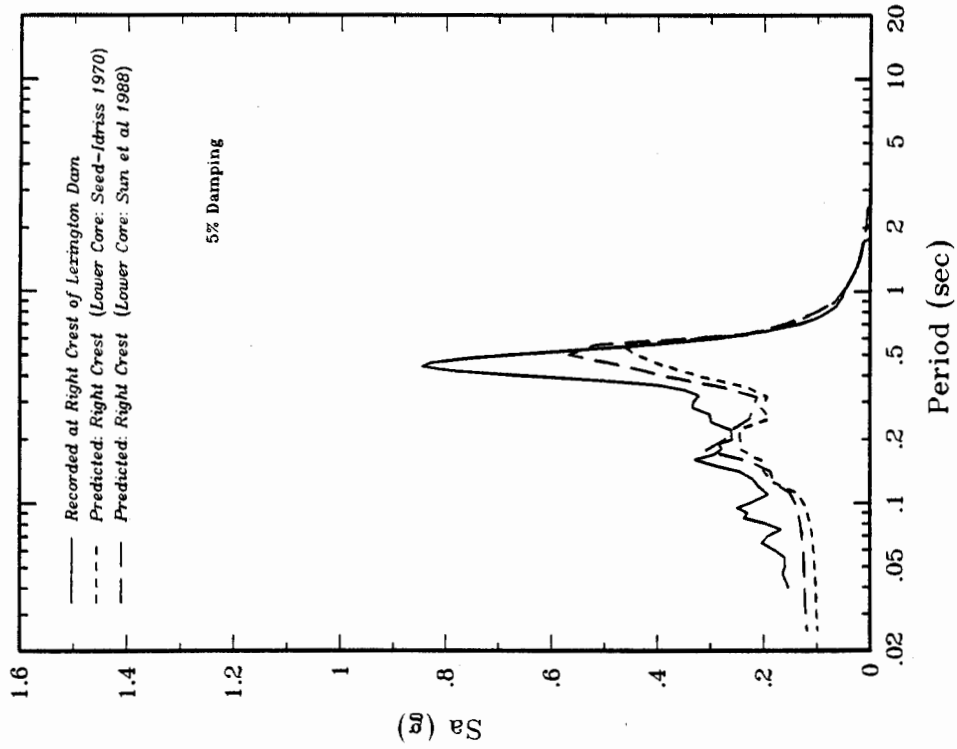


Figure 20: Modulus and Damping Relationships Used in Response Analyses of Lexington Dam

(a) Lake Elisman Event (8/8/89)
 $M_L = 5.2$



(b) Loma Prieta Event (10/17/89)
 $M_L = 7.0$

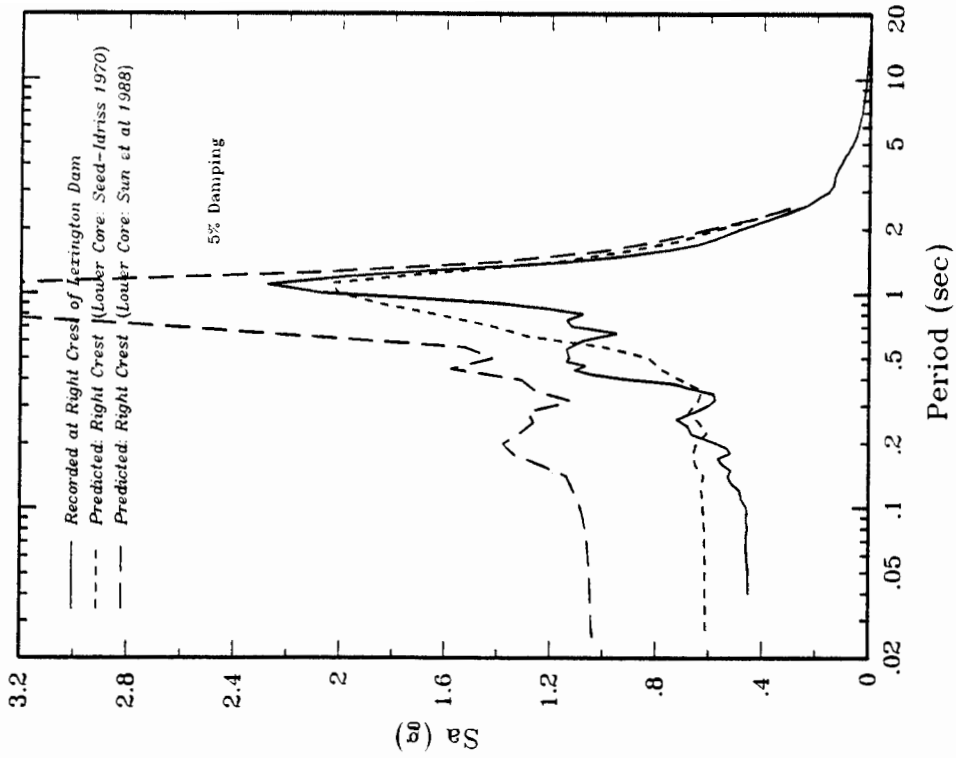


Figure 21: Comparison of Recorded Response at Crest of Lexington Dam with That Computed for Two Modulus Reduction Relationships

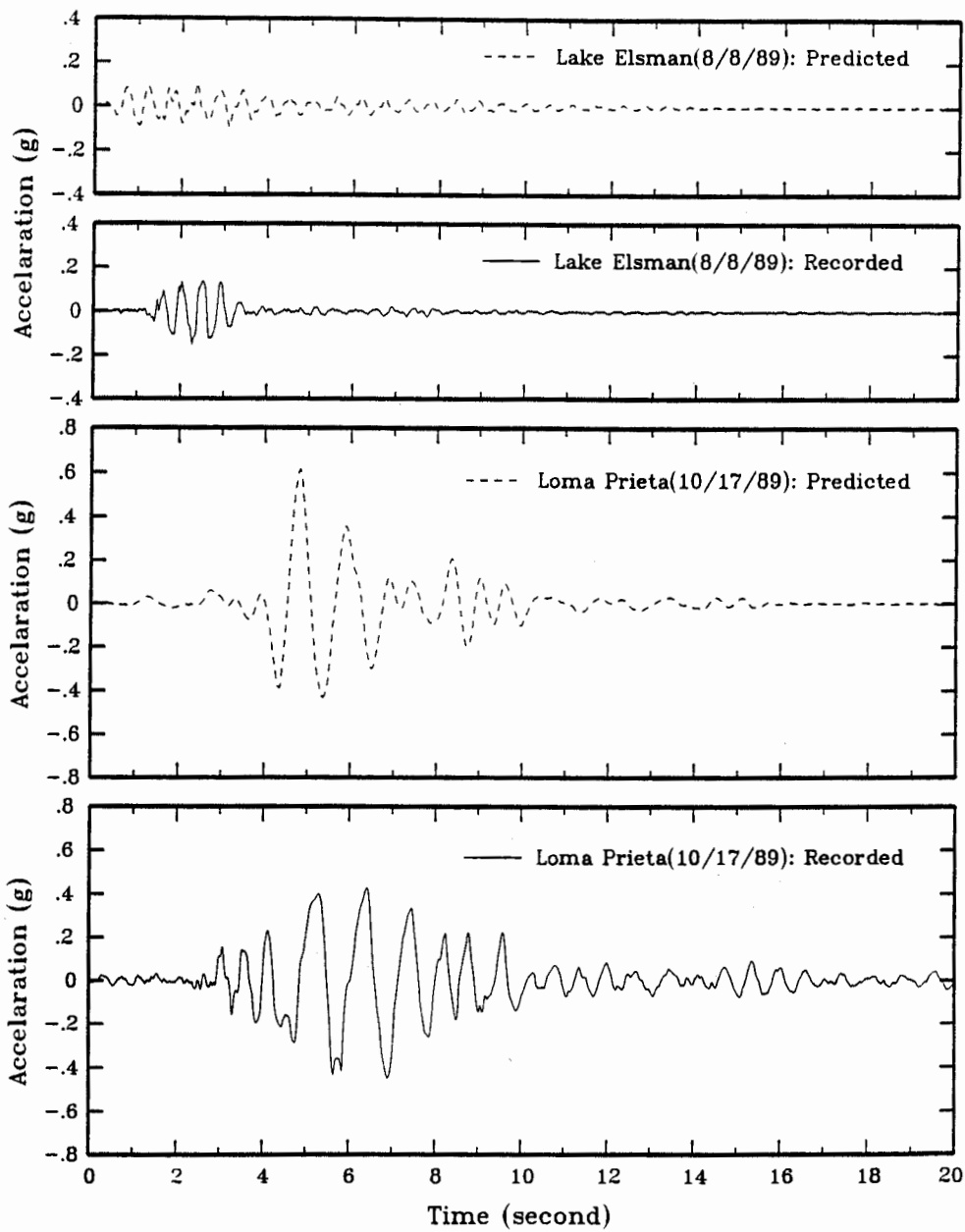
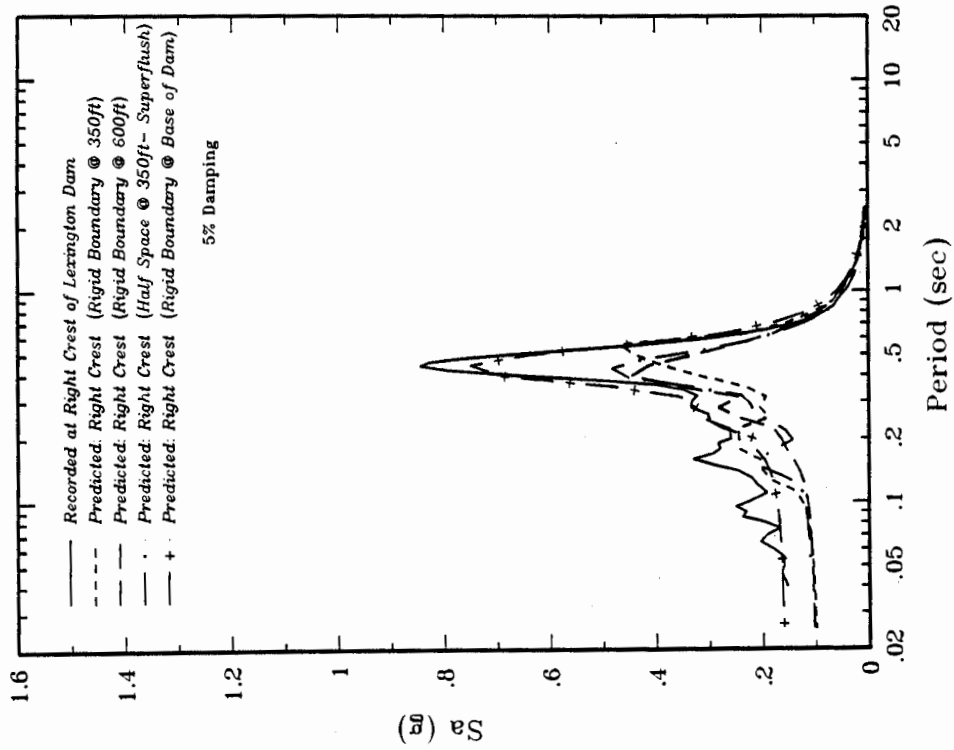


Figure 22: Comparison Between Computed and Recorded Acceleration Time-Histories at Crest of Lexington Dam

(a) Lake Elisman Event (8/8/89)
 $M_L=5.2$



(b) Loma Prieta Event (10/17/89)
 $M_L=7.0$

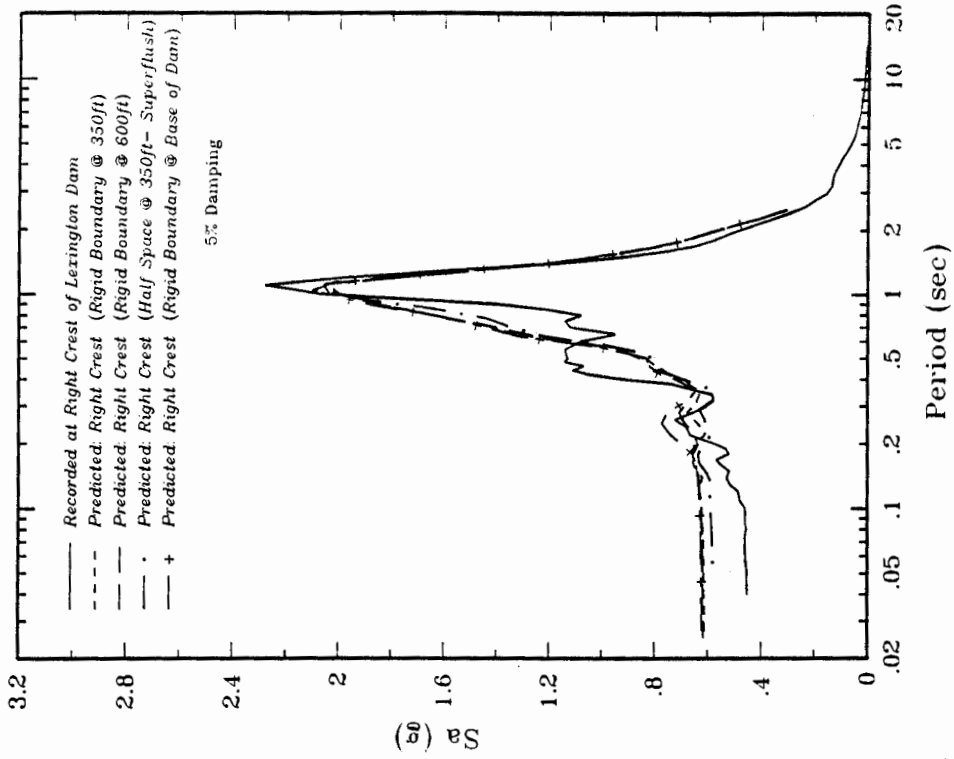


Figure 23: Effects of Location of Rigid Boundary on the Response at the Crest of Lexington Dam

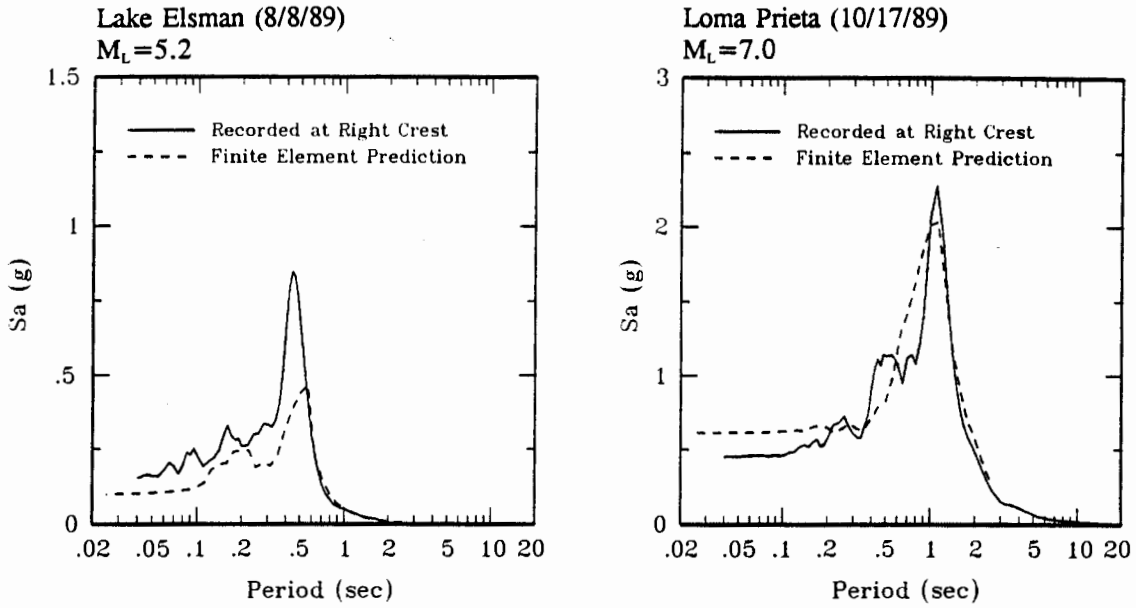


Figure 24: Comparison of Computed and Recorded Response Spectra at Crest of Lexington Dam (Transverse Component, 5% Damping)

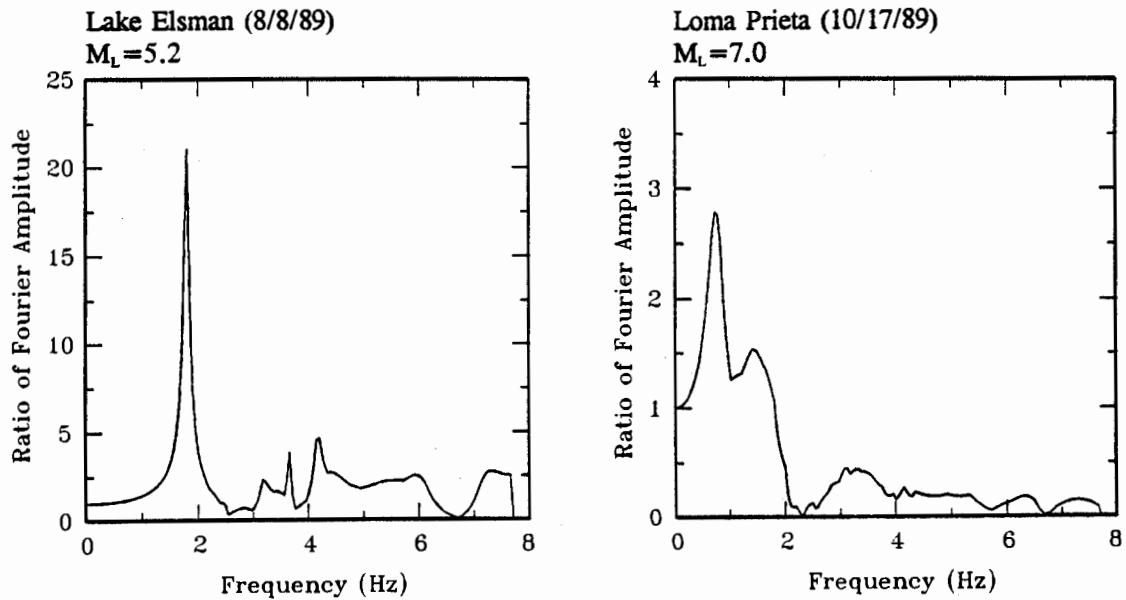


Figure 25: Computed Fourier Amplitude Transfer Functions (Crest to Left Abutment) at Lexington Dam

Plotted values are for elements at embankment centerline extending between crest and foundation level

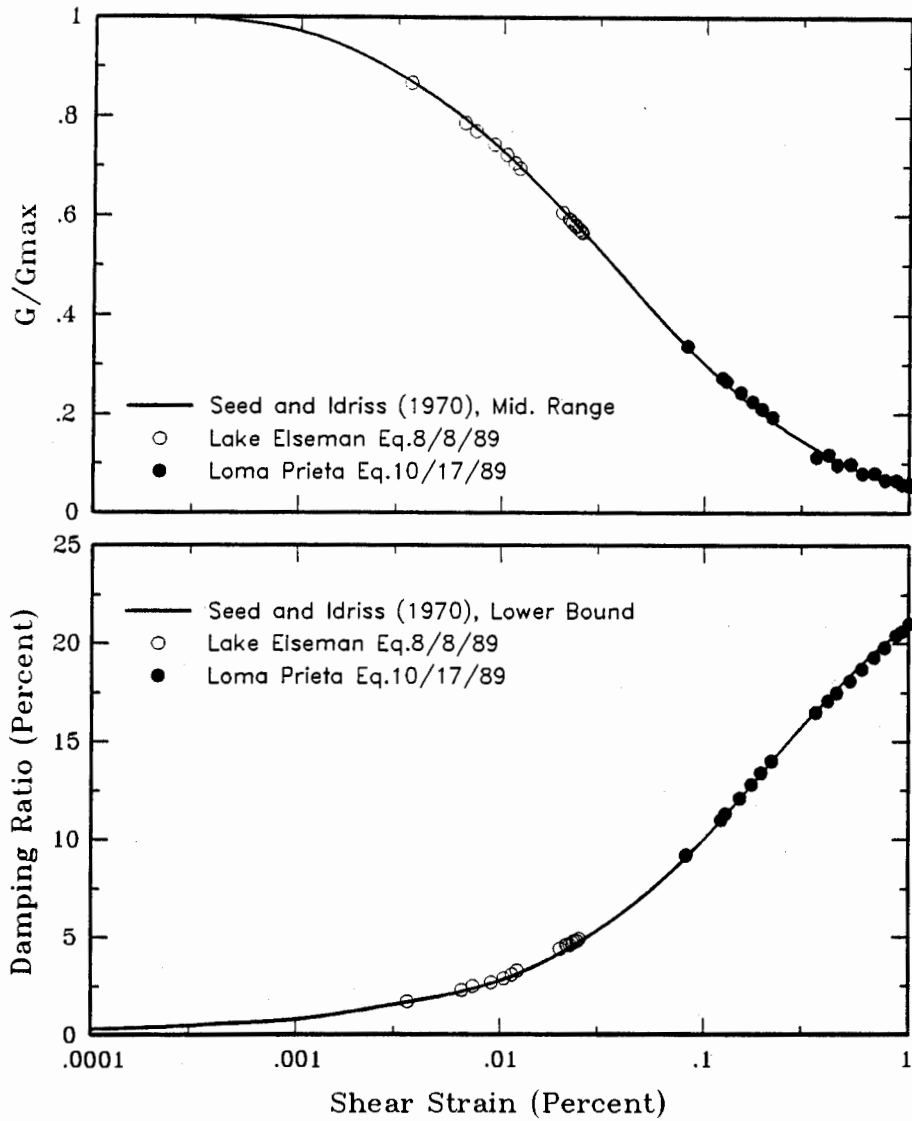
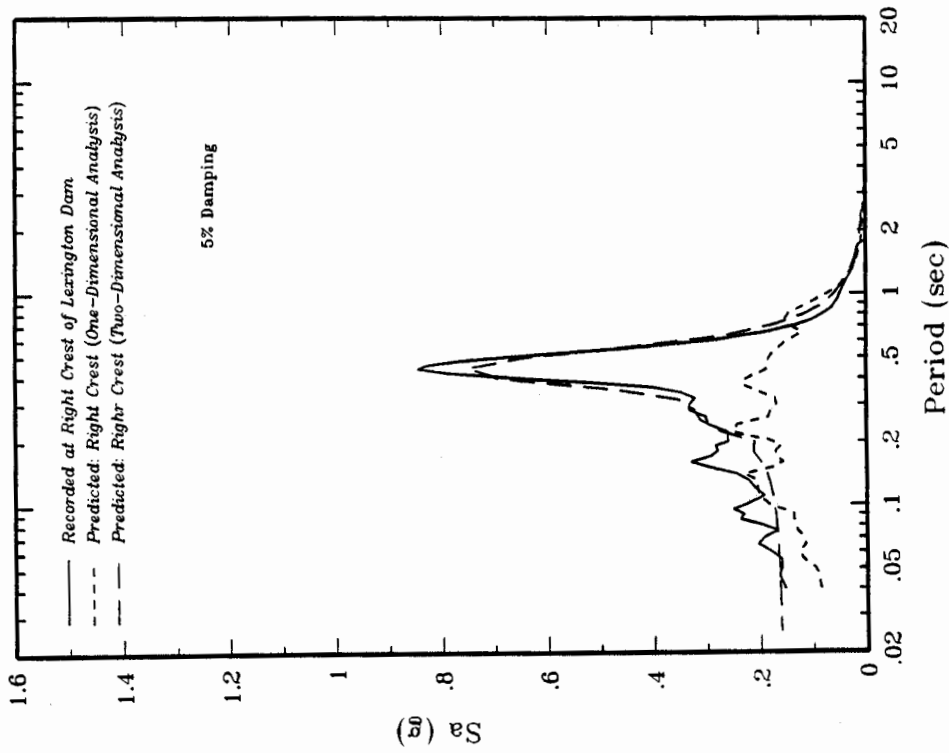


Figure 26: Variation of Shear Modulus and Damping with Strain for Two Ground Shaking Levels at Lexington Dam

(a) Lake Elsman Event (8/8/89)
 $M_L=5.2$



(b) Loma Prieta Event (10/17/89)
 $M_L=7.0$

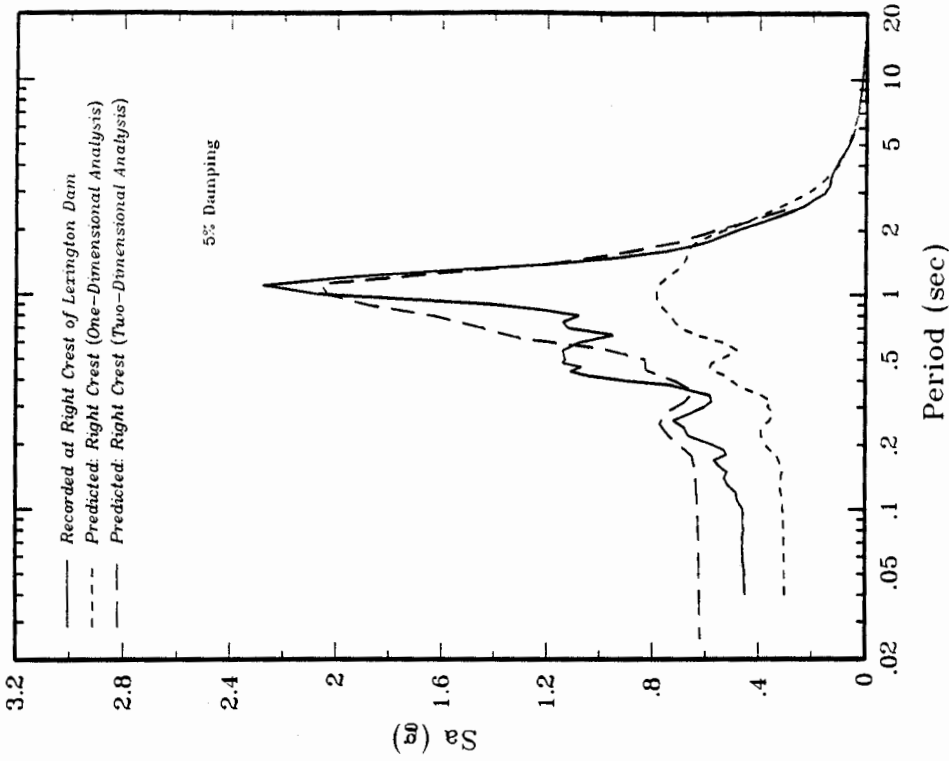


Figure 27: Comparison of Computed One- and Two-Dimensional Response at the Crest of Lexington Dam with Recorded Ground Motions (Transverse Component, 5% Damping)

5 SUMMARY AND CONCLUSIONS

The recorded responses of Lexington Dam during the Loma Prieta earthquake and two smaller events provided an opportunity to evaluate the applicability of commonly used dynamic response analysis procedures as well as to evaluate the nonlinear, strain-dependent behavior of the embankment soils during various levels of ground shaking.

Analyses of response and Fourier spectral ratios of the recorded motions, as well as one- and two-dimensional response studies, provided insight into the behavior of the embankment materials during various levels of earthquake shaking. The primary conclusions of this study are summarized as follows.

- a) Response and Fourier spectral ratios (crest to abutment) of the recorded ground motions showed a definite shift in the fundamental natural period of the embankment with increased level of shaking, demonstrating a nonlinear strain-dependent behavior of the embankment soils at the level of shaking associated with the Loma Prieta earthquake.
- b) Two-dimensional finite element analyses of the embankment response, using equivalent linear, strain-dependent material properties, provided predictions of ground motions at the crest of the dam that are in reasonable agreement with recorded motions.
- c) For the maximum shear modulus values obtained from measured shear wave velocities, the modulus reduction curve representing the mid-range curve of the Seed and Idriss (1970) relationship for sands and their lower bound curve for damping provided results that best matched the recorded motions.

- d) The two-dimensional finite-element computations using input ground motions associated with the Loma Prieta earthquake revealed a nonlinear strain dependent behavior of the embankment soils with estimated reduction in shear modulus of the order of about 60% to 95% of the initial low strain values.

- e) For cases in which the ratio of shear wave velocity of the foundation bedrock to that of the embankment material is low (less than 8), assuming a rigid rock boundary at the base of the dam may not prove reasonable for computing the response at the crest.

- f) The use of one-dimensional analyses to approximate the two-dimensional embankment response provided poor agreement with recorded motions and with results of two-dimensional finite element analyses.

Current guidelines for the evaluation of seismic stability of high embankment dams, located in active seismic environments, require the use of two-dimensional dynamic finite element analyses for estimating the embankment response. The analyses performed in this study showed that currently used dynamic analyses procedures, using the equivalent linear method to model the nonlinear strain dependent behavior of the embankment material, can provide response estimates that are in reasonable agreement with the recorded data.

REFERENCES

- Chang, C.-Y., Power, M.S., Tang, Y.K., and Mok, C.-M., 1989, Evidence of nonlinear soil response during a moderate earthquake: Proceedings of the Twelfth International Conference on Soil Mechanics and Foundation Engineering, Rio de Janeiro, Brazil, August 13-18.
- Gazetas, G., and Dakoulas, P., 1991, Aspects of seismic analysis and design of rockfall dams--state of the art paper: Proceedings of the Second International Conference on Recent Advances in Geotechnical and Earthquake Engineering and Soil Dynamics, Vol. II, March.
- Lysmer, J., Udaka, T., Tsai, C.-F., and Seed, H.B., 1975, FLUSH--a computer program for approximate 3-D analysis of soil-structure interaction problems: Earthquake Engineering Research Center, Report No. EERC 75-30, University of California, Berkeley, November.
- Pacific Gas and Electric Company, 1988, Long-term seismic program: Final Report submitted to the Nuclear Regulatory Commission, July.
- Schnabel, P.B., Lysmer, J., and Seed, H.B., 1972, SHAKE--a computer program for earthquake response analysis of horizontally layered sites: Earthquake Engineering Research Center, Report No. EERC 72-12, University of California, Berkeley, December.
- Seed, H.B., and Idriss, I.M., 1970, Soil moduli and damping factors for dynamic response analysis: Earthquake Engineering Research Center, Report No. EERC 70-10, University of California, Berkeley.
- Seed, H.B., Wong, R.T., Idriss, I.M., and Tokimatsu, K., 1984, Moduli and damping factors for dynamic analyses of cohesionless soils: Earthquake Engineering Research Center, Report No. UCB/EERC 84/14, University of California, Berkeley, September.
- Shakal, A., Huang, M., Reichle, M., Ventura, C., Cao, T., Sherburne, R., Savage, M., Daragh, R., and Peterson, C., 1989, CSMIP strong-motion records from the Santa Cruz Mountains (Loma Prieta), California, earthquake of 17 October 1989: California Strong Motion Instrumentation Program, Report No. OSMS 89-06, 195 p.
- Sun, J.I., Golesorkhi, R., and Seed, H.B., 1988, Dynamic moduli and damping ratios for cohesive soils: Earthquake Engineering Research Center, Report No. UCB/EERC 88/15, University of California, Berkeley.
- Volpe, R.L. & Associates, 1990, Investigation of SCVWD Dams affected by the Loma Prieta earthquake of October 17, 1989, March.
- Udaka, T., 1989, Super FLUSH Users Guide: Earthquake Engineering Technology, San Ramon, California.
- Wahler Associates, 1982, Seismic safety evaluation of Lexington Dam: Final Report Submitted to Santa Clara Valley Water District, May.